MODELLING, SIMULATION & SPEED CONTROL OF FIVE-PHASE INDUCTION MOTOR USING INDIRECT FIELD ORIENTATION CONTROL(IFOC) METHOD

A thesis submitted in partial fulfillment
Of the requirements for the degree of

Master of Electrical Engineering

By

Utpal Nath

Examination Roll No: M4ELE1606
Class Roll No: 01410802007
Reg. No: 128894 of 2014-15

Under the Supervision of

Prof. Debashis Chatterjee

Department of Electrical Engineering
Faculty of Engineering and Technology
Jadavpur University
Kolkata – 700 032

2016

Declaration of Originality and Compliance of Academic Ethics

I hereby declare that this thesis contains literature survey and original research work by the undersigned candidate, as a part of his Master of Electrical Engineering studies.

All information in this document have been obtained and presented in accordance with academic rules and ethical conduct.

I also declare that, as required by these rules and conduct, I have fully cited and referred all materials and results that are not original to this work.

Name: Utpal Nath

Exam. Roll No. : M4ELE1606

Thesis Title: MODELLING,SIMULATION & SPEED CONTROL OF FIVE- PHASE INDUCTION MOTOR USING INDIRECT FIELD ORIENTATION CONTROL(IFOC) METHOD

____

Signature with Date

Department of Electrical Engineering
Jadavpur University

CERTIFICATE

This is to certify that the thesis entitled "MODELLING,SIMULATION & SPEED CONTROL OF FIVE-PHASE INDUCTION MOTOR USING INDIRECT FIELD ORIENTATION CONTROL(IFOC) METHOD". Submitted by Utpal Nath in partial fulfillment of the requirements for the award of Master of Engineering Degree in Electrical Engineering at Jadavpur University, Kolkata is a work carried out by him under my supervision and guidance. To the best of my knowledge, the matter embodied in the thesis has not been submitted to any other University / Institute for the award of any degree or diploma.

____

[Dr. Debashis Chatterjee]
Professor
Dept. of Electrical Engineering
Jadavpur University
Kolkata-700032

Countersigned by

____

Head of the Department
Electrical Engineering Department
Jadavpur University
Kolkata- 700 032

____

Dean of the Faculty of
Engineering and Technology
Jadavpur University
Kolkata -700 032

Department of Electrical Engineering
Jadavpur University

CERTIFICATE OF APPROVAL*

The foregoing thesis is hereby approved as a creditable study of an engineering subject carried out and presented in a satisfactory manner to warrant its acceptance as pre-requisite to the degree for which it has been submitted. It is notified to be understood that by this approval, the undersigned do not necessarily endorse or approve any statement made, opinion expressed and conclusion drawn therein but approve the thesis only for the purpose for which it has been submitted.

Final Examination for the
Evaluation of the thesis

Board of Examiners

1. ____________________

2. ____________________

* Only in case the thesis is approved

Acknowledgement

On the submission of my thesis on "***Modelling, Simulation and Speed Control of Five-phase induction motor using Indirect Field Orientation Control (IFOC) method***", I would like to articulate my deep gratitude and sincere thanks to my supervisor **Prof. Debashis Chatterjee** of Electrical Department, Jadavpur University, Kolkata for his most valuable guidance and thoughtful suggestions during the course of my work throughout the year. His help and advice has been a constant source of inspiration.

I am sincerely thankful to **Prof. Swapan Kr. Goswami,** Head of the Department, Electrical Engg. and all the faculty members for providing a solid background for my studies and research thereafter.

I am thankful to Mr. Arunava Chatterjee, Research Scholar of Electrical Engineering Department for providing me with the necessary guidance and support for carrying out this thesis. An assemblage of this nature could never have been attempted without reference to and inspiration from the works of others whose details are mentioned in reference section. I acknowledge my indebtedness to all of them.

I am thankful to all my classmates and the department research scholars for their cooperation and unfailing help during the project work. I am grateful to all my friends who made my stay in Jadavpur, an unforgettable and rewarding experience.

Signature

Abstract

Since 19th century, three-phase Induction motors are the starting point to design an electrical drive system which is widely used in many industrial applications. In late 1960s, multiphase induction machine is developed and used in many applications like ship propulsion system, hybrids motor as multiphase drive several advantage over conventional three induction machine drives. The advantage are: reducing the amplitude and increasing the frequency of torque pulsations, reducing the rotor harmonic currents, reducing the current per phase without increasing the voltage per phase, lowering the dc-link current harmonics, and higher reliability.

In modern control theory, different mathematical models describe induction motor according to the employed control methods. Vector control strategy can be applied to this electrical motor type in symmetrical three phase version or in unsymmetrical two phase version. The operation of the induction motor can be analyzed similar to a DC motor through this control method.

Using Kron's Dynamic machine model, the mathematical model for five phase induction machine is developed considering the fundamental flux only. With these technological projections, various command approaches have been developed by the scientific community to master in real time. In electrical control system, the indirect field oriented control (IFOC) scheme being one of the most recent steps in this direction. In this control scheme the electromagnetic torque and net flux magnitude are estimated from direct axis and quadrature axis stator currents reference and depends on motor parameters.

In this thesis, a simple and straightforward IFOC scheme has been developed for a five phase induction motor and conventional IFOC scheme has been simulated with *MATLAB Simulink* and SIMSCAPE tools and evaluate the performance of motor quantities under various speed and load. Literature review has been done to study the recent improvements in multiphase induction machine, application areas and various control schemes and its advantage.

TABLE OF CONTENTS

List of principle symbols

In general, symbols are defined locally. The list of principle symbols used in the thesis is given below:

$d^e - q^e$	synchronously rotating reference frame direct and quadrature axis
d^s - q^s	Stationary reference frame direct and quadrature axis
$i_{dr}{}^s$, $i_{qr}{}^s$	$d^s - q^s$ axes rotor current
$i_{ds}{}^s$, $i_{qs}{}^s$	$d^s - q^s$ axes stator current
i_{dr}, i_{qr}	$d^e - q^e$ axes rotor current
i_{ds}, i_{qs}	$d^e - q^e$ axes stator current
J	Moment of inertia (kg-m^2)
X_{ds}	d^e – axis synchronous reactance
X_{qs}	q^e – axis synchronous reactance
X_{lr}	rotor leakage reactance
X_{ls}	stator leakage reactance
θ_e	Angle of synchronously rotating frame
θ_r	rotor angle
θ_{sl}	slip angle
T_r	Time Constant
L_r	Rotor inductance
L_s	Stator inductance
L_{lr}	Rotor leakage inductance
L_{ls}	Stator leakage inductance
L_{dm}	d^e – axis magnetizing inductance
L_{qm}	q^e – axis magnetizing inductance
R_s	Stator resistance

R_r	Rotor resistance
S	Slip
T_e	Developed Torque
T_L	Load Torque
$V_{dr}{}^s$, $V_{qr}{}^s$	$d^s - q^s$ axes rotor voltage
$V_{ds}{}^s$, $V_{qs}{}^s$	$d^s - q^s$ axes rotor voltage
V_{dr}, V_{qr}	$d^e - q^e$ axes rotor voltage
V_{ds}, V_{qs}	$d^e - q^e$ axes stator voltage
Ψ_r	rotor flux linkage
Ψ_s	stator flux linkage
$\Psi_{dr}{}^s$, $\Psi_{qr}{}^s$	$d^s - q^s$ rotor flux linkage
$\Psi_{ds}{}^s$, $\Psi_{qs}{}^s$	$d^s - q^s$ stator flux linkage
Ψ_{dr}, Ψ_{qr}	$d^e - q^e$ rotor flux linkage
Ψ_{ds}, Ψ_{qs}	$d^e - q^e$ stator flux linkage
ω_e (or ω)	stator or line frequency
ω_m	rotor mechanical speed
ω_r	rotor electrical speed
ω_{sl}	slip speed
p	differentiation with respect to time ($\frac{d}{dt}$)

List of Figures

CHAPTER 1

1. Introduction

1.1 Induction machine

In the last few decades, induction motor has been recognized as a workhouse in the industry primarily due to the advantages of: rugged brushless construction, less maintenance, lower cost, robustness and no separate need for DC field. Nearly 80% of world's ac motors are induction motors. The disadvantages of both DC machines and synchronous machine are eliminated in the induction machine. The induction machine also has drawbacks of developing low torque, drawing heavy starting current, high per phase current during fault and having no easy means of speed control. Though induction motors do not inherently have the capability of variable speed operation. Due to this reason, earlier dc motors were applied in most of the electrical drives. But the recent developments in speed control methods of the induction motor have led to their large scale use in almost all electrical drives. Out of the several methods of speed control of an induction such as pole changing, frequency variation, variable rotor resistance, variable stator voltage, constant *V/f* control, slip power recovery scheme etc. The closed loop constant *V/f* speed control method is most widely used. In this method, the *V/f* ratio is kept constant which in turn maintains the magnetizing flux constant so that the maximum torque remains unchanged. Thus, the motor is completely utilized in this method [1].

During starting of an induction motor, the stator resistance and the motor inductance (both rotor and stator) must be kept low to reduce the steady state time and also to reduce the jerks during starting. On the other hand, higher value of rotor resistance leads to lesser jerks while having no effect on the steady state time. The vector control analysis of an induction motor allows the decoupled analysis where the torque and the flux components can be independently controlled (just as in dc motor) [2]-[4]. This makes the analysis easier than the per phase equivalent circuit. In

1969, the concept of multiphase induction machine is first developed and design to reduce the per phase current during fault, toque ripple, etc.

1.2 Five-phase induction machine

Multiphase machines have been first introduced in late 1960s. They are widely used in variable speed applications like aerospace, transportation, electric ship propulsion, hybrid electric vehicles and textile industry. The advantages of multiphase machine over general three-phase machine are, reducing the current per phase without variation of supply voltage, increased fault tolerance level, reducing the rotor harmonic currents, reducing the amplitude and increasing the frequency of torque pulsation thus results higher torque density and reliability. Meanwhile, the disadvantage is that the drive system is complex and hence a bit costly.

Many researchers claim that torque per ampere increased with the increased of phase number for a certain machine volume. Thus results a rapid pace of development in multiphase motor drive area. Multiphase induction machines have been mainly used in high power and/or high current applications required multi leg inverter supply. The power rating of the converter should meet the required level of the machine and load. However, the converter ratings cannot be increased over a certain range due to the limitation of the power rating of semiconductor devices. One solution to this problem is using multi-level inverter, where switches of reduced rating are employed to develop high power level converters. The advent of inverter fed-motor drives also removed the limits of the number of motor phases. This fact allows designing machines with more than three-phases and emphasizes investigation and applications of multi-phase motor drives.

The aim of this thesis is to design and implement a speed control scheme of 5-phase induction motor drive system using Indirect Field Orientation Control method (IFOC). This type field orientation control demonstration that an induction motor can be controlled like a dc motor. IFOC method is very popular in industrial application. In IFOC, initially rotor flux estimation is carried out; along with unit vector signals are generated in feed-forward manner. In short, the control system of the drive calculates the corresponding current component references from the flux and torque references given by the drive's speed control. Typically, proportional-integral (PI) controllers are used to keep the measured current components at their reference values. This type of vector control makes the speed control of induction machine smooth speed regulation and high dynamic performance [5]-[8].

1.2.1 Review of Relevant Literature

The induction machine, invented independently by Nikola Tesla and Galileo Ferraris in 1889, represents a well-established technology. The primary advantage of the induction machine is the rugged brushless construction that does not need a separate DC field excitation makes it highly reliable and less maintenance. Basic property, induction motors will accelerate their loads from rest and will run without producing a twice line-frequency pulsating torque. Machines having more than three phases exhibit the same properties, but those with one or two phases do not. Thus three-phase induction machine is adopted universally in electrical power system. In general, during the six step operation of three-phase inverter operation, one particular problem at the time was the low frequency torque ripple. Since the lowest frequency torque ripple harmonic in an n-phase machine is caused by the time harmonics of the supply of the order 2n+1 (its frequency is 2n times higher than the supply frequency), an increase in the number of phases of the machine appeared as the best solution to the problem. Hence significance effort of introducing five-phase or six-phase variable speed drive is introduced. Many researchers point out several reasons to upsurge of interest in multiphase induction machine systems. The chief advantages are,

(i) In multiphase phase machine, stator excitation produce field contains lower space harmonics, thus efficiency is increased.

(ii) Higher fault tolerance, as if one phase is open-circuit in 9-phase induction machine, still it will be self-starting.

(iii) Pulsating torque is produce at even multiple of fundamental, thus increased the dynamic response.

In late 1960s, primary introduction and investigation of multiphase variable drive is studied in [9]. However multiphase induction motor required power from multiphase power electronics converter, the input stage of converter is connected to three-phase supply. The output stage of the converter and the stator winding of the motor must have the same number of phases, but provided this simple requirement is met, any number of phases may be used. The multiphase inverter analysis is studied in [08]. The variable speed drive using five-phase and six-phase using VSI and CSI is introduce in [10]-[14].

In 1990s, research started on the application area of multiphase variable speed drives [15]-[20]. In [21] –[25], H. A. Toliyat, G. K .Singh and E. Levi make some complimentary review on multi-phase induction machine at 20th century. At the same time, d-q model of five-phase synchronous reluctance machine considering the third harmonics is explain in [42]. Speed control of five –phase induction machine using Indirect field orientation control method considering the space harmonics and DSP based controlled studied is describe in [26]-[29] and fuzzy logic control of five-phase induction machine explain in [41]. The torque density improvement, fault tolerance capability, efficiency and multi-motor control to improve the drive system performance is presented in [30] – [40].The model of control scheme of five phase induction is design by T A. Lipo and H.A. Toliyat in [31]- [32]. The dual plane vector control of five-phase induction machine is studied in [43] explain that each space harmonics can be excited separately. In [44], G.K. Singh and V. Pant explain that the reliability and performance of 5-phase induction machine can be increased by phase redundancy process. Modeling and analysis of five-phase induction machine under fault condition due to unbalance condition and open-circuit is explain in [45]-[46].

1.3 Principles of Vector Control

Before 1970s, the scalar control method voltage fed and current fed methods are mostly used. Scalar control method is very simple to implement, but inherent coupling effect cause instability due to higher order harmonics and reduce dynamic response of the system in induction machine drives.

After 1970s, the vector control is introduced by Darmstadt's K. Hasse and Siemens' Blaschke. This method is mostly used in speed control of AC machines drive as its can be used as separately excited DC motor by decoupling the flux and toque of the AC machine 90 degree to each other, it is also called as transvector or orthogonal control As the use of micro-computer or DSP is mandatory, its make control circuit a complex one.

In vector control, an AC induction or synchronous motor is controlled under all operating conditions like a separately excited DC motor. That is, the AC motor behaves like a DC motor in which the field flux linkage and armature flux linkage created by the respective field and armature (or torque component) currents are orthogonally aligned such that, when torque is controlled, the field flux linkage is not affected, hence enabling dynamic torque response.

Because of the inherent coupling problem, an induction motor cannot generally give such fast response. DC machine like performance can also be extended to an induction motor if the machine control is considered in a synchronously rotating reference frame (d^e-q^e) where the sinusoidal variables appear as dc quantities in steady state. In Fig. 1.1, the induction motor with the Inverter drives and vector control in the input site is shown with two control current inputs as i_{ds}* and i_{qs}*. These current are direct axis component and quadrature axis component of stator in rotating frame. In vector control, i_{ds} is analogous to field current and i_{qs} is analogous to armature current of a dc machine. This means that when i_{qs}* is controlled, it affects the actual i_{qs} current only, but does not affect the flux in d-axis and when i_{ds}* is controlled, it controls the flux only and does not affect the i_{qs} component of current. Thus three-phase (a, b, c) is converted to two-phase (d-q) in this control.

In short, vector control makes correct orientation of current in any condition of induction machine controlled [2]-[3].

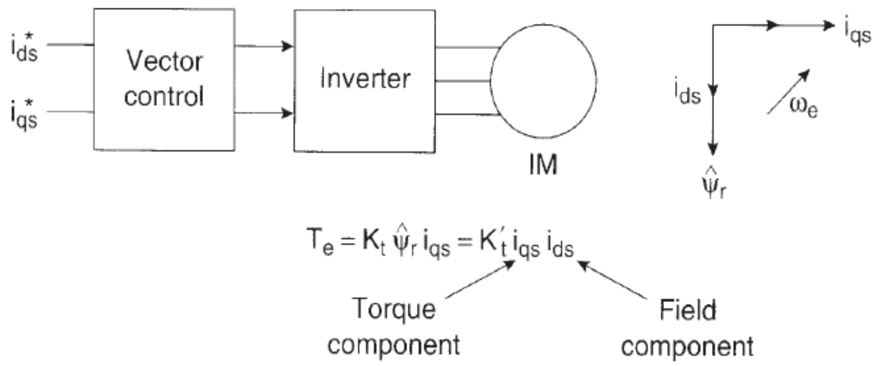

Fig.1.1. Vector control of induction motor.

1.4 Three-phase to Two-phase Transformation

In variable speed drive, the drive system within a feedback loop, therefore transient behavior along with steady state condition is taken under consideration. Vector control is based on d-q model of the system. Basically, it's a conversion of three phase to two phase (*abc – dq*) in stationary stator frame than into arbitrary rotating frame. The concept of *d-q* model is mandatory to understand the principle of Vector Control in [2]-[3].

Basically, induction machine is a transformer with rotating secondary. Here, the coupling coefficient per phase of rotor and stator change with rotor position. The machine equation can be developed as differential equation and matrix form containing self or mutual inductance and resistance respectively. In the Fig. 1.2, the three phase machine can be represented as a equivalent two-phase machine where d^s, q^s, d^r and q^r are the direct and quadrature axis component in stator and rotor on induction machine displace by an angle θ_r.

In 1920s, R. H. Park proposed a new theory of electric machine analysis to solve this problem. He formulated a change of variables which, in effect, replaced the variables (voltages, currents and flux linkages) associated with the stator windings of a synchronous machine with variables associated with fictitious windings rotating with the rotor at synchronous speed.

Essentially, he transformed, the stator variables to a synchronously rotating reference frame fixed in the rotor. With such a transformation (called Park's transformation). He showed that all the time-varying inductances that occur due to an electric circuit in relative motion and electric circuits with varying magnetic reluctances can be eliminated. Later, in the l930s, H. C. Stanley showed that time-varying inductances in the voltage equations of an induction machine due to electric circuits in relative motion can be eliminated by transforming the rotor variables to variables associated with fictitious stationary windings. In this case, the rotor variables are transformed to a stationary reference frame fixed on the stator. Later, G. Kron proposed a transformation of both stator and rotor variables to a synchronously rotating reference frame that moves with the rotating magnetic field. This model is extremely important and will be discussed later in detail in thesis.

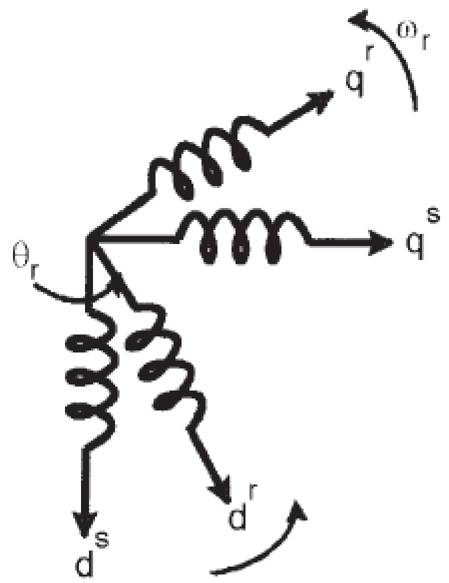

Fig.1.2. *d-q* axes equivalent two phase machine.

Later, in 1940s, D. S. Brereton proposed a transformation of stator variables to a rotating reference frame that is fixed on the rotor. In fact, it was shown later by Krause and Thomas that time-varying inductances can be eliminated by referring the stator and rotor variables to a common reference frame which may rotate at any speed (arbitrary reference frame).

1.4.1 Axis Conversion

Consider a balanced 3-phase system phase displaced by 120^0 to each other. Our aim is to transform the three-phase stationary reference frame (*as-bs-cs*) variables into two-phase stationary reference frame (d^s-q^s) variable and then transform those to synchronously rotating reference frame (d^e-q^e) and vice versa.

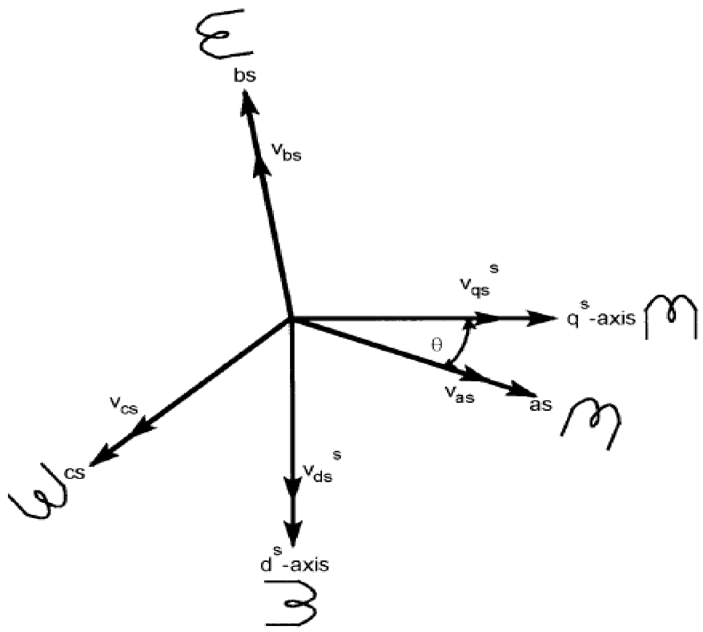

Fig.1.3. Stationary frame *a-b-c* to d^s-q^s axis conversion.

In the Figure 1.3, the d^s-q^s axes are displaced by an angle θ. The voltage matrix formed by v_{as}-v_{bs}-v_{cs} resolved in terms of $v_{ds}{}^s$ and $v_{qs}{}^s$ as,

$$\begin{bmatrix} v_{as} \\ v_{bs} \\ v_{cs} \end{bmatrix} = \begin{bmatrix} \cos\theta & \sin\theta & 1 \\ \cos(\theta-120^o) & \sin(\theta-120^o) & 1 \\ \cos(\theta+120^o) & \sin(\theta+120^o) & 1 \end{bmatrix} \begin{bmatrix} v_{qs}^s \\ v_{ds}^s \\ v_{os}^s \end{bmatrix} \tag{1.1}$$

The inverse matrix form in shown below,

$$\begin{bmatrix} v_{qs}^s \\ v_{ds}^s \\ v_{os}^s \end{bmatrix} = \frac{2}{3} \begin{bmatrix} \cos\theta & \cos(\theta-120^o) & \cos(\theta+120^o) \\ \sin\theta & \sin(\theta-120^o) & \sin(\theta+120^o) \\ 0.5 & 0.5 & 0.5 \end{bmatrix} \begin{bmatrix} v_{as} \\ v_{bs} \\ v_{cs} \end{bmatrix} \tag{1.2}$$

Here, v_{os} is represents as zero sequence component. It can be neglected in many matrix forms for simplicity. The current and flux linkage equation can deduce by similar manner. For simplicity θ is set to 0^0, it means that *as* axis is coincident with q^s axis. Ignoring the zero sequence component, the transformations are,

$$v_{as} = v_{qs}{}^{s} \tag{1.3}$$

$$v_{bs} = \frac{1}{2} v_{qs}{}^{s} - \frac{\sqrt{3}}{2} v_{ds}{}^{s} \tag{1.4}$$

$$v_{cs} = \frac{1}{2} v_{qs}{}^{s} + \frac{\sqrt{3}}{2} v_{ds}{}^{s} \tag{1.5}$$

By taking the inverse,

$$v_{qs}{}^{s} = v_{as} \tag{1.6}$$

$$v_{ds}{}^{s} = -\frac{1}{\sqrt{3}} v_{bs} + \frac{1}{\sqrt{3}} v_{bs} \tag{1.7}$$

Fig. 1.4 shows the synchronously rotating d^e-q^e axes, which rotate at synchronous speed ω_e with respect of d^s-q^s with an angle $\theta_e = \omega_e t$ The two-phase d^s-q^s axis are transformed into the hypothetical windings mounted on the d^e-q^e axes. The voltages on the d^s-q^s axes can be converted into the d^e-q^e frame as follows,

$$v_{qs}{}^{e} = v_{qs}{}^{s} cos\theta_e - v_{ds}{}^{s} sin\theta_e \tag{1.8}$$

$$v_{ds}{}^{e} = v_{qs}{}^{s} cos\theta_e + v_{ds}{}^{s} sin\theta_e \tag{1.9}$$

Now, the resolving the rotating frame parameter in stationary frame, the equation becomes,

$$v_{qs}{}^{s} = v_{qs}{}^{e} cos\theta_e + v_{ds}{}^{e} sin\theta_e \tag{1.10}$$

$$v_{ds}{}^{s} = -v_{qs}{}^{e} cos\theta_e + v_{ds}{}^{e} sin\theta_e \tag{1.11}$$

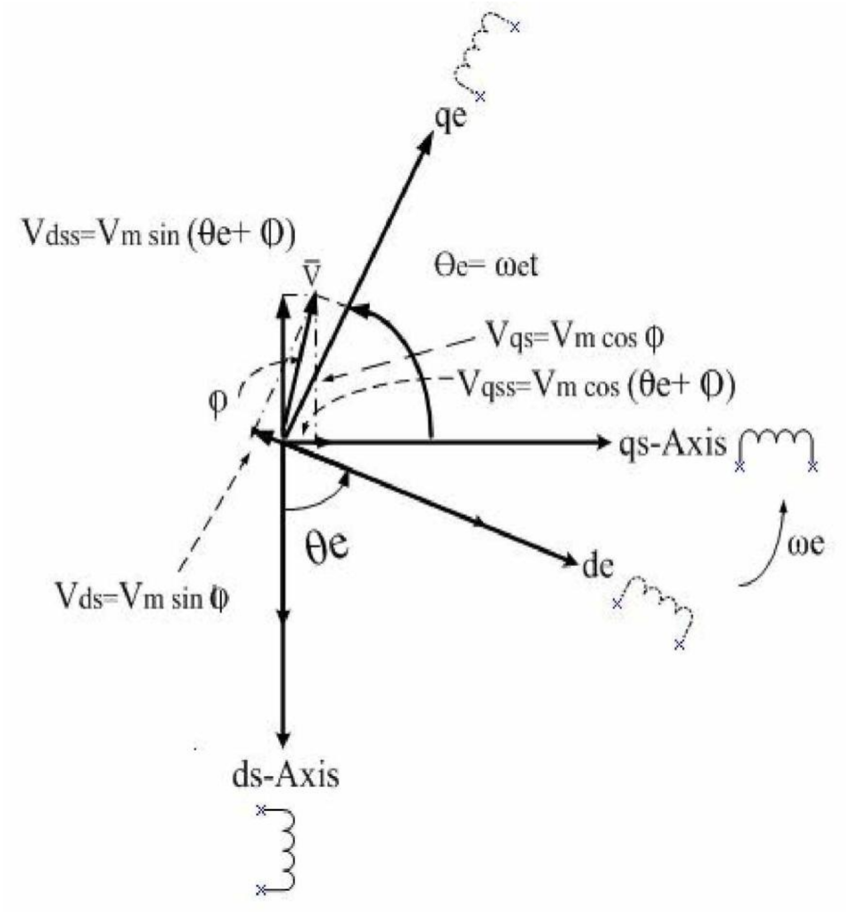

Fig.1.4. Transformation of stationary frame (d^s-q^s) to synchronous rotating frame (d^e-q^e).

Assuming a balanced three-phase supply is given as *as-bs-cs*, than after some substitution from equation, show that the two phase voltage as $v_{ds}{}^{e}$ and $v_{qs}{}^{e}$ are balanced and 90^0 out of phase with peak value. The summarized equations are,

$$V_{qs}{}^{e} = V_m cos\phi \tag{1.12}$$

$$V_{ds}{}^{e} = -V_m sin\phi \tag{1.13}$$

From the equation 1.2 and 1.3 ,one can conclude that a sinusoidal variable in stationary frame can be appear as dc values in synchronously rotating reference frame. Thus stator and rotor circuit variable can be determined. In fact, it is not mandatory that stator variable to be balanced, it may be any arbitrary time function.

1.5 Dynamic Model of Induction Machine by Kron's Equations

For the two-phase machine shown in Figure 1.1, we need to represent both d^s -q^s and d^r - q^r circuits and their variables in a synchronously rotating d^e - q^e frame. One may write the following stator and rotor voltage equations as,

$$v_{qs}{}^{s} = R_s i_{qs}{}^{s} + p\psi_{qs}{}^{s} \tag{1.14}$$

$$v_{ds}{}^{s} = R_s i_{ds}{}^{s} + p\psi_{ds}{}^{s} \tag{1.15}$$

$$0 = R_{dr} i_{dr}^{s} + p\psi_{dr}^{s} + \omega_r \psi_{qr}^{s} \tag{1.16}$$

$$0 = R_{qr} i_{qr}^{s} + p\psi_{qr}^{s} - \omega_r \psi_{dr}^{s} \tag{1.17}$$

Where, $\psi_{qs}{}^{s}$, $\psi_{ds}{}^{s}$ and $\psi_{qr}{}^{s}$, $\psi_{dr}{}^{s}$ are q-axis and d-axis stator and rotor flux linkages respectively. For a singly-fed machine, such as a cage rotor motor, rotor voltages are zero. When above equations are converted to d^e-q^e frame, then the following equations can be written in synchronously rotating frame,

$$v_{qs}^{e} = R_{qs} i_{qs}^{e} + p\psi_{qs}^{e} + \omega_e \psi_{ds}^{e} \tag{1.18}$$

$$v_{ds}^{e} = R_{ds} i_{ds}^{e} + p\psi_{ds}^{e} - \omega_e \psi_{qs}^{e} \tag{1.19}$$

Where, all the variables and parameters are referred to the stator. Since the rotor actually moves at speed ω_e, the d-q axes fixed on the rotor move at a speed $(\omega_e - \omega_r)$ relative to the synchronously rotating frame. Therefore, in d^e-q^e frame, the rotor equations are,

$$0 = R_{qr} i_{qr}^{e} + p\psi_{qr}^{e} + \left(\omega_e - \omega_r\right)\psi_{dr}^{e} \tag{1.20}$$

$$0 = R_{dr} i_{dr}^{e} + p\psi_{qr}^{e} + \left(\omega_e - \omega_r\right)\psi_{dr}^{e} \tag{1.21}$$

Figure 1.5 shows the d^e-q^e dynamic model equivalent circuits that satisfy equations (1.18) - (1.21). The advantage of the d^e-q^e dynamic model of the machine is that all the sinusoidal variables in stationary frame appear as dc quantities in synchronous frame, as explain earlier. The flux linkage equations in term of current from Fig. 1.5 are

$$\psi_{qs} = L_{ls} i_{qs} + L_m \left(i_{qs} + i_{qr} \right) \tag{1.22}$$

$$\psi_{qr} = L_{lr} i_{qr} + L_m \left(i_{qs} + i_{qr} \right) \tag{1.23}$$

$$\psi_{qm} = L_m \left(i_{qs} + i_{qr} \right) \tag{1.24}$$

$$\psi_{ds} = L_{ls} i_{ds} + L_m \left(i_{ds} + i_{dr} \right) \tag{1.25}$$

$$\psi_{dr} = L_{ls} i_{dr} + L_m \left(i_{ds} + i_{dr} \right) \tag{1.26}$$

$$\psi_{dm} = L_m \left(i_{ds} + i_{dr} \right) \tag{1.27}$$

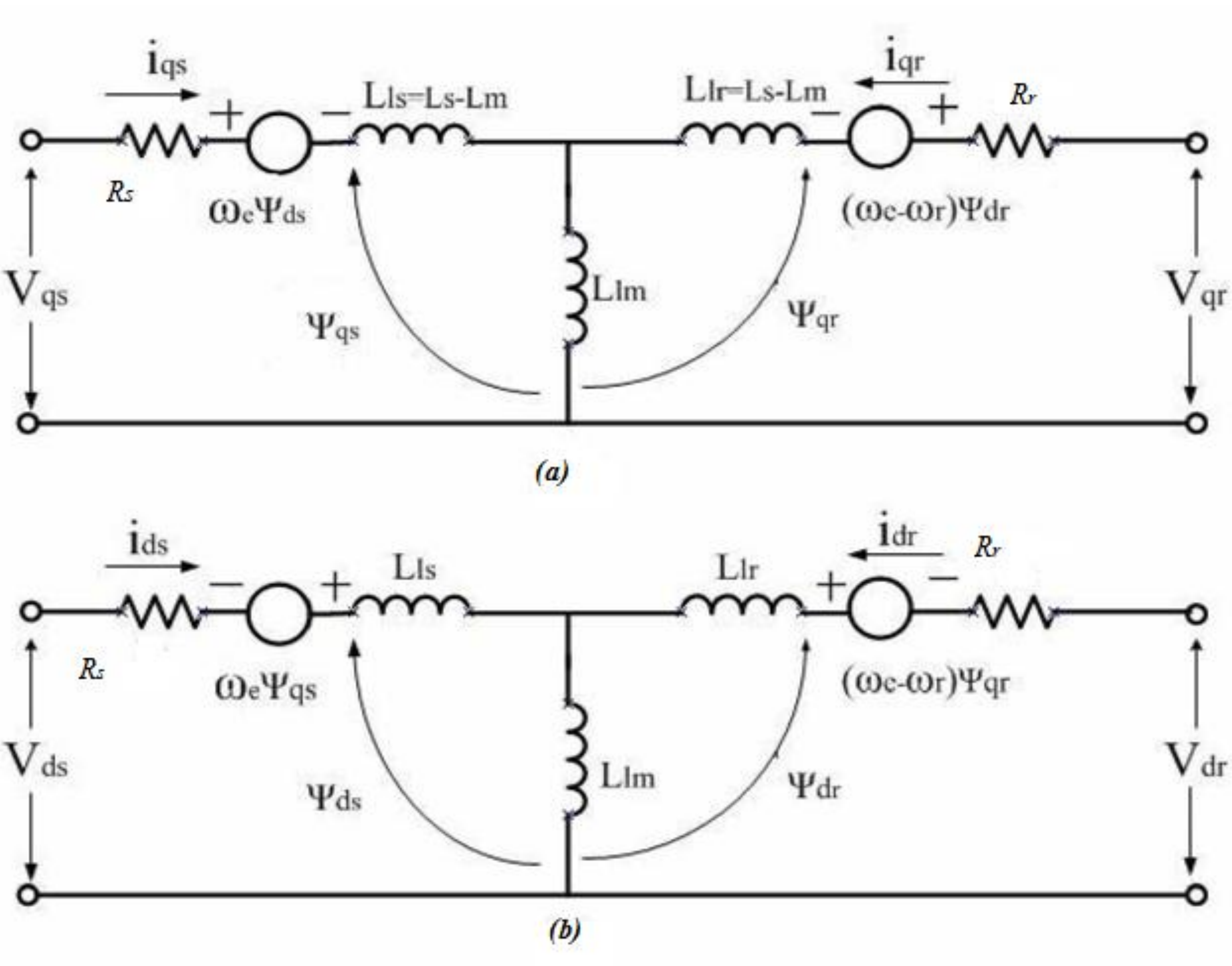

Fig.1.5. Dynamic d^e - q^e equivalent circuits of machine (a) q^e- axis circuit, (b) d^e - axis circuit.

Combining the voltage and flux expressions, the electrical transient model for induction machine in terms of voltages and currents can be given in matrix form as,

$$\begin{bmatrix} v_{qs} \\ v_{ds} \\ 0 \\ 0 \end{bmatrix} = \begin{bmatrix} R_s + sL_s & \omega_e L_s & sL_m & \omega_e L_m \\ -\omega_e L_s & R_s + sL_s & -\omega_e L_m & sL_m \\ sL_m & (\omega_e - \omega_r)L_m & R_r + sL_r & (\omega_e - \omega_r)L_r \\ -(\omega_e - \omega_r)L_m & sL_m & -(\omega_e - \omega_r)L_r & R_r + sL_r \end{bmatrix} \begin{bmatrix} i_{qs} \\ i_{ds} \\ i_{qr} \\ i_{dr} \end{bmatrix} \tag{1.28}$$

Where, *s* is the Laplace operator. If the speed ω_e, is considered constant (infinite inertia load), the electrical dynamics of the machine are given by a fourth-order linear system. Then, knowing the inputs v_{qs}, v_{ds} and ω_e, the currents i_{qs}, i_{ds}, i_{qr} and i_{dr} can be solved from equation (1.26). If the machine is fed by current sources are independent. Then, the dependent variables can be solved from equation (1.26). The rotor speed ω_r, in equation (1.26) cannot normally be treated as a constant. It can be related to the torques as,

$$T_e = T_L + Jp\omega_m = T_L + \frac{2}{P} Jp\omega_r \tag{1.29}$$

The Figure 1.6 shows the complex equivalent circuit in rotating frame where $v_{qdr} = 0$. Note that the steady state equations can always be derived by substituting the time derivative components to zero. The steady-state equations can be derived as from the Figure 1.6

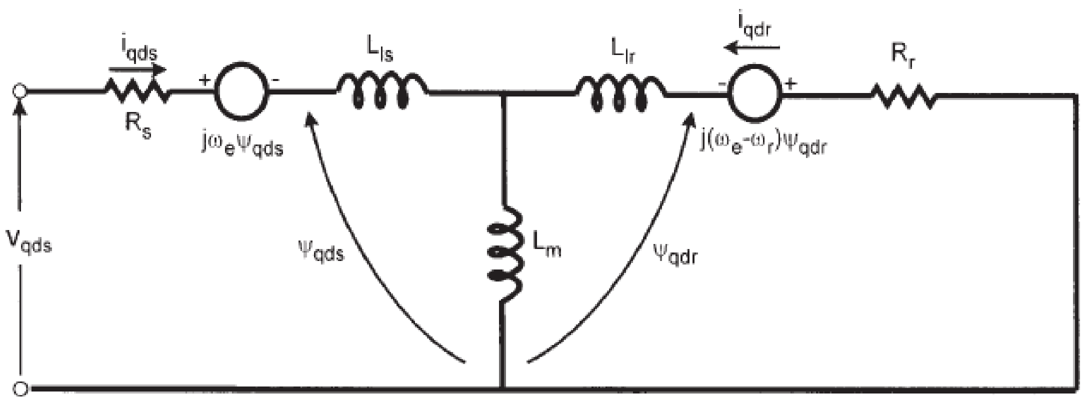

Fig.1.6. Complex synchronous frame *dqs* equivalent circuit.

$$V_s = R_s I_s + j\omega_e \psi_s \tag{1.30}$$

$$0 = \frac{R_s}{s} I_r + j\omega_e \psi_r \tag{1.31}$$

Where the complex vectors are replaced by the corresponding *rms* phasors. These equations satisfy the generalized steady-state equivalent circuit of induction machine.

In general, torque is developed by the interaction of air gap flux and rotor mmf in induction machine. It will be expressed in more general form, relating the *d*-*q* components of variables. The torque can he generally expressed in the vector form as,

$$T_e = \frac{3}{2}\left(\frac{P}{2}\right)\psi_m X\, I_r \tag{1.32}$$

Resolving the variable into d^e -q^e component as shown in Figure. 1.7,

$$T_e = \frac{3}{2}\left(\frac{P}{2}\right)(\psi_{dm} i_{qr} - \psi_{qm} i_{dr}) \tag{1.33}$$

$$= \frac{3}{2}\left(\frac{P}{2}\right) L_m (i_{qs} i_{dr} - i_{ds} i_{qr}) \tag{1.34}$$

$$= \frac{3}{2}\left(\frac{P}{2}\right)(\psi_{dr} i_{qr} - \psi_{qr} i_{dr}) \tag{1.35}$$

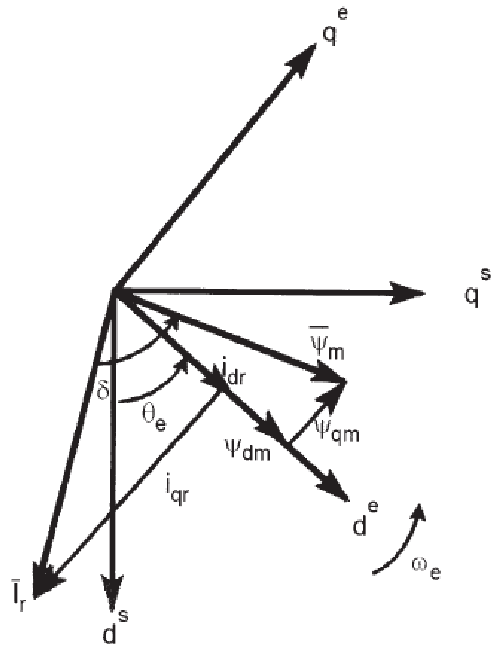

Fig.1.7. Flux and current vector in d^e -q^e frame.

Equations (1.26), (1.27) and (1.33) give the complete model of the electro-mechanical dynamics of an induction machine in synchronous frame [4]. Using this Kron’s dynamic model of three-phase machine, the dynamic model of five-phase induction machine is designed and explained in this thesis using *MATLAB Simulink* and *SimPowerSystems* toolbox.

CHAPTER 2

2. Model of Five-Phase of Induction machine

2.1 Mathematical model of five-phase induction motor

A two-pole five-phase induction machine with identical phase windings, which are evenly distributed with a 72^{o} angle between them and with each phase occupying four stator slots is shown in Fig.2.1.

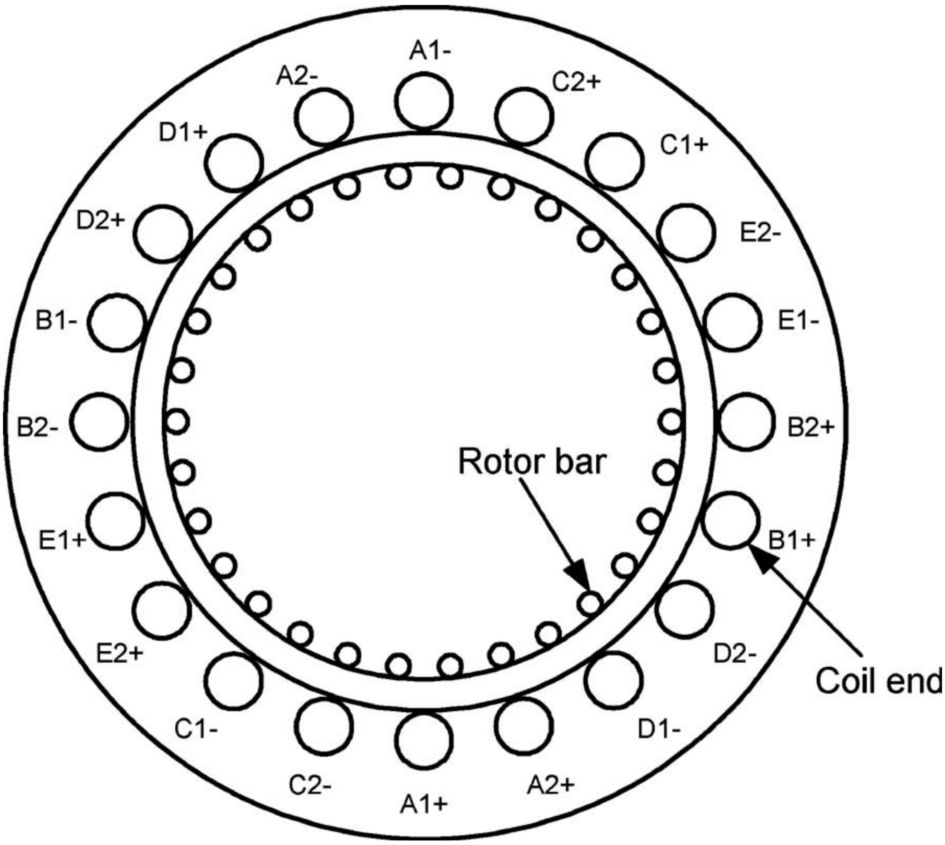

Fig 2.1.Cross sectional view of a five-phase machine with windings.

For the five phase machine, the stator *as-bs-cs-ds-es* voltages can be converted into $d_1-q_1-d_3-q_3-n$ arbitrary reference frame by,

$$\begin{bmatrix} v_{as} \\ v_{bs} \\ v_{cs} \\ v_{ds} \\ v_{es} \end{bmatrix} = \sqrt{\frac{2}{5}} \begin{bmatrix} \cos\theta_{e1} & \cos\left(\theta_{e1}-\frac{2\pi}{5}\right) & \cos\left(\theta_{e1}-2\left(\frac{2\pi}{5}\right)\right) & \cos\left(\theta_{e1}-3\left(\frac{2\pi}{5}\right)\right) & \cos\left(\theta_{e1}-4\left(\frac{2\pi}{5}\right)\right) \\ -\sin\theta_{e1} & -\sin\left(\theta_{e1}-\frac{2\pi}{5}\right) & -\sin\left(\theta_{e1}-2\left(\frac{2\pi}{5}\right)\right) & -\sin\left(\theta_{e1}-3\left(\frac{2\pi}{5}\right)\right) & -\sin\left(\theta_{e1}-4\left(\frac{2\pi}{5}\right)\right) \\ \cos 3\theta_{e3} & \cos\left(3\theta_{e3}-3\left(\frac{2\pi}{5}\right)\right) & \cos\left(3\theta_{e3}-\frac{2\pi}{5}\right) & \cos\left(3\theta_{e3}-4\left(\frac{2\pi}{5}\right)\right) & \cos\left(3\theta_{e3}-2\left(\frac{2\pi}{5}\right)\right) \\ -\sin 3\theta_{e3} & -\sin\left(3\theta_{e3}-3\left(\frac{2\pi}{5}\right)\right) & -\sin\left(3\theta_{e3}-\frac{2\pi}{5}\right) & -\sin\left(3\theta_{e3}-4\left(\frac{2\pi}{5}\right)\right) & -\sin\left(3\theta_{e3}-2\left(\frac{2\pi}{5}\right)\right) \\ \frac{1}{\sqrt{2}} & \frac{1}{\sqrt{2}} & \frac{1}{\sqrt{2}} & \frac{1}{\sqrt{2}} & \frac{1}{\sqrt{2}} \end{bmatrix} \begin{bmatrix} v_{ds1} \\ v_{qs1} \\ v_{ds3} \\ v_{qs3} \\ v_{ns} \end{bmatrix} \tag{2.1}$$

Similar expressions hold true for stator currents also. By vector space decomposition, the first and third space harmonics of the machine are modeled in the $d_1-q_1-d_3-q_3-n$ arbitrary reference frame. This model is similar to that in [32] and [33].

A. The machine in the $d_1 - q_1$ vector plane,

$$V_{d1s} = R_s i_{d1s} + p\psi_{d1s} - \omega_{e1}\psi_{q1s} \tag{2.2}$$

$$V_{q1s} = R_s i_{q1s} + p\psi_{q1s} + \omega_{e1}\psi_{d1s} \tag{2.3}$$

$$0 = R_{r1} i_{d1r} + p\psi_{d1r} - (\omega_{e1} - \omega_r)\psi_{q1r} \tag{2.4}$$

$$0 = R_{r1} i_{q1s} + p\psi_{q1r} + (\omega_{e1} - \omega_r)\psi_{d1r} \tag{2.5}$$

Where,

$$\psi_{d1s} = (L_{ls} + L_{m1})i_{d1s} + L_{m1}i_{d1r} \tag{2.6}$$

$$\psi_{q1s} = (L_{ls} + L_{m1})i_{q1s} + L_m i_{q1r} \tag{2.7}$$

$$\psi_{d1r} = (L_{ls} + L_{m1})i_{d1r} + L_{m1}i_{d1s} \tag{2.8}$$

$$\psi_{q1r} = (L_{ls} + L_m)i_{q1r} + L_m i_{q1s} \tag{2.9}$$

B. Machine in the $d_3 - q_3$ vector plane,

$$V_{d3s} = R_s i_{d3s} + p\psi_{d3s} - 3\omega_{e3}\psi_{q3s} \tag{2.10}$$

$$V_{q3s} = R_s i_{q3s} + p\psi_{q3s} + 3\omega_{e3}\psi_{d3s} \tag{2.11}$$

$$0 = R_{r3} i_{d3r} + p\psi_{d3r} - 3(\omega_{e3} - \omega_r)\psi_{q3r} \tag{2.12}$$

$$0 = R_{r1} i_{q3r} + p\psi_{q3r} + 3(\omega_{e3} - \omega_r)\psi_{d3r} \tag{2.13}$$

Where,

$$\psi_{d3s} = (L_{3s} + L_{m3}) i_{d3s} + L_{m3} i_{d3r} \tag{2.14}$$

$$\psi_{q3s} = (L_{ls} + L_{m3}) i_{q3s} + L_m i_{q3r} \tag{2.15}$$

$$\psi_{d3r} = (L_{ls} + L_{m3}) i_{d3r} + L_{m3} i_{d3s} \tag{2.16}$$

$$\psi_{q3r} = (L_{ls} + L_m) i_{q3r} + L_m i_{q3s} \tag{2.17}$$

In (2.2) - (2.17), R_s and L_{ls} are stator resistance and stator leakage inductance. $R_{r1\,(3)}$ and $L_{lr1(3)}$ are stator referred rotor resistance and rotor leakage inductance. $L_{m1(3)}$ is the magnetizing inductance. The subscript number indicates the associated vector plane. ω_{e1}, ω_{e3} are the rotating speeds of the d_1-q_1 and d_3-q_3 axes, and ω_r is the rotor angular speed. p is the differential operator. The electromagnetic torque can be derived from the partial variation of the co-energy with respect to rotor angular position,

$$T_e = \frac{P}{2} [L_{m1}(i_{q1s} i_{d1r} - i_{d1s} i_{q1r}) + 3L_{m3}(i_{q3s} i_{d3r} - i_{d3s} i_{q3r})] \tag{2.18}$$

In [26], the machine model is represent as fundamental flux component along with third order harmonics as they acquire orthogonal property between the vectors planes (d_1-q_1 & d_3-q_3). The higher order harmonics are mapped into the d_1-q_1 and d_3-q_3 vector plane. In this thesis, only the first space harmonics (fundamental component of flux) is taken in consideration. The model is similar to that in [41]. At first the *as-bs-cs-ds-es* five phase stator voltages are converted into stationary d^s-q^s axes voltage components as,

$$\begin{bmatrix} v_{as} \\ v_{bs} \\ v_{cs} \\ v_{ds} \\ v_{es} \end{bmatrix} = \frac{2}{5} \begin{bmatrix} \cos\theta_e & \cos\left(\theta_e - \frac{2\pi}{5}\right) & \cos\left(\theta_e - 2\left(\frac{2\pi}{5}\right)\right) & \cos\left(\theta_e + 2\left(\frac{2\pi}{5}\right)\right) & \cos\left(\theta_e + \frac{2\pi}{5}\right) \\ \sin\theta_e & \sin\left(\theta_e - \frac{2\pi}{5}\right) & \sin\left(\theta_e - 2\left(\frac{2\pi}{5}\right)\right) & \sin\left(\theta_e + 2\left(\frac{2\pi}{5}\right)\right) & \sin\left(\theta_e + \frac{2\pi}{5}\right) \\ \cos 3\theta_e & \cos 3\left(\theta_e - \frac{2\pi}{5}\right) & \cos 3\left(\theta_e - 2\left(\frac{2\pi}{5}\right)\right) & \cos 3\left(\theta_e + 2\left(\frac{2\pi}{5}\right)\right) & \cos 3\left(\theta_e + \frac{2\pi}{5}\right) \\ \sin 3\theta_e & \sin 3\left(\theta_e - \frac{2\pi}{5}\right) & \sin 3\left(\theta_e - 2\left(\frac{2\pi}{5}\right)\right) & \sin 3\left(\theta_e + 2\left(\frac{2\pi}{5}\right)\right) & \sin 3\left(\theta_e + \frac{2\pi}{5}\right) \\ \frac{1}{\sqrt{2}} & \frac{1}{\sqrt{2}} & \frac{1}{\sqrt{2}} & \frac{1}{\sqrt{2}} & \frac{1}{\sqrt{2}} \end{bmatrix} \begin{bmatrix} v_{ds} \\ v_{qs} \\ 0 \\ 0 \\ 0 \end{bmatrix} \tag{2.19}$$

Where, the third space harmonic stationary components are equated to zero as shown in (2.19). The general equation of five-phase induction motor in stationary d^s-q^s reference frame is given by equations (1.14) – (1.15). The flux linkage equations are,

$$\psi_{qs} = L_{ls} i_{qs} + L_m \left(i_{qs} + i_{qr} \right) \tag{2.20}$$

$$\psi_{ds} = L_{ls} i_{ds} + L_m \left(i_{ds} + i_{dr} \right) \tag{2.21}$$

$$\psi_{qr} = L_{lr} i_{qr} + L_m \left(i_{qr} + i_{qs} \right) \tag{2.22}$$

$$\psi_{dr} = L_{lr} i_{dr} + L_m \left(i_{dr} + i_{ds} \right) \tag{2.23}$$

The electromagnetic torque equation is expressed as,

$$T_e = \frac{5}{2}\left(\frac{P}{2}\right)(\psi_{ds} i_{qs} - \psi_{qs} i_{ds}) \tag{2.24}$$

$$T_e - T_l = J \frac{d\omega}{dt} + B\omega_r \tag{2.25}$$

2.2 Modeling of a five-phase system

A balanced AC five phase system will consist of five individual sinusoidal phases which are displaced in space by 72^o electrical degrees. The five-phase voltages can be represented mathematically as,

$$V_a = V_m \sin(\omega t)$$

$$V_b = V_m \sin\left(\omega t - \frac{2\pi}{5}\right)$$

$$V_c = V_m \sin\left(\omega t - 2\left(\frac{2\pi}{5}\right)\right) \tag{2.24}$$

$$V_d = V_m \sin\left(\omega t + 2\left(\frac{2\pi}{5}\right)\right)$$

$$V_e = V_m \sin\left(\omega t + \frac{2\pi}{5}\right)$$

The equation (2.24) can be represented in *MATLAB/Simulink* using the *Sine wave source block* as shown in Fig. 2.2 (a) below. The output is shown in Fig. 2.2 (b).

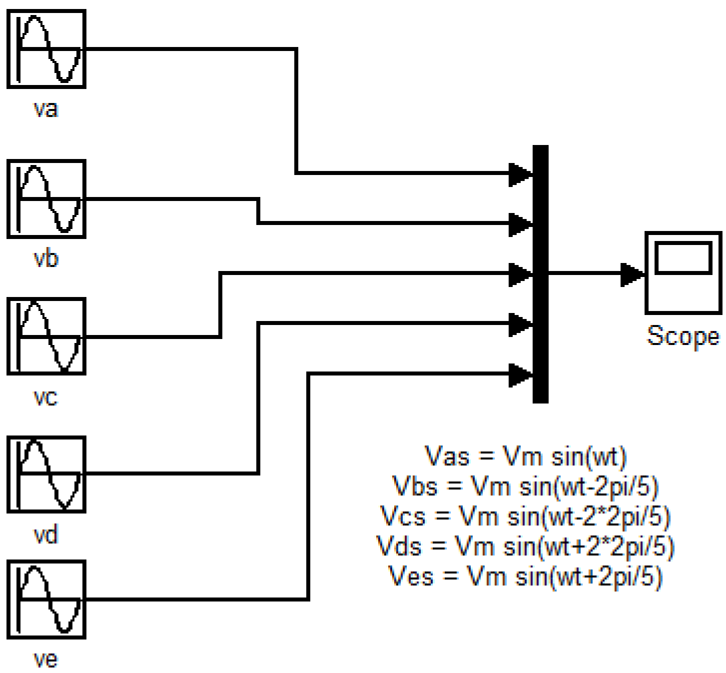

(a)

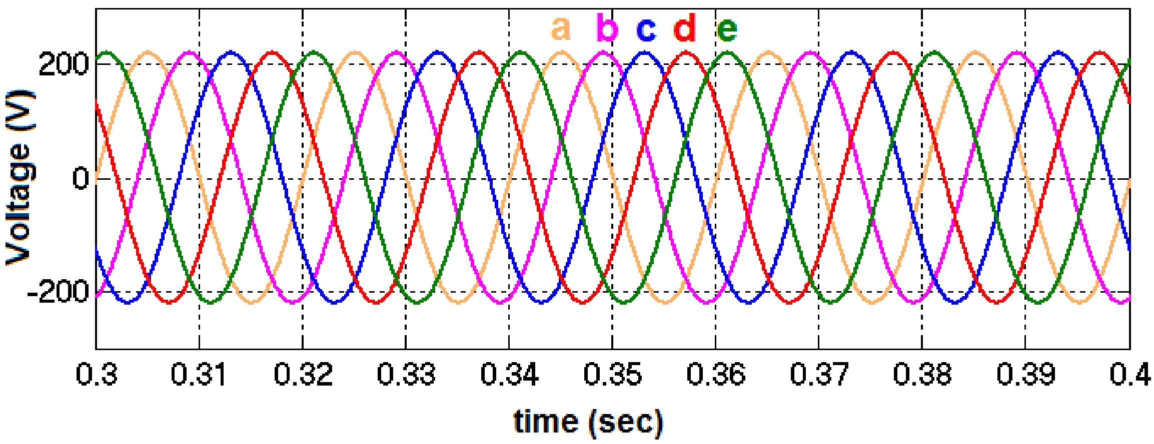

(b)

Fig. 2.2. (a) Five-phase supply and (b) five-phase voltage waveform.

The above model can be used in *Simulink* to supply a five-phase machine with balanced windings. The five phase induction modeling is discussed in the next section.

2.3 Modeling of proposed five-phase induction machine

The five-phase induction machine is modeled using the stationary d^s-q^s axes equations (2.20)-(2.25) and (1.14)-(1.17). The five-phase induction machine model is shown in Fig. 2.3.

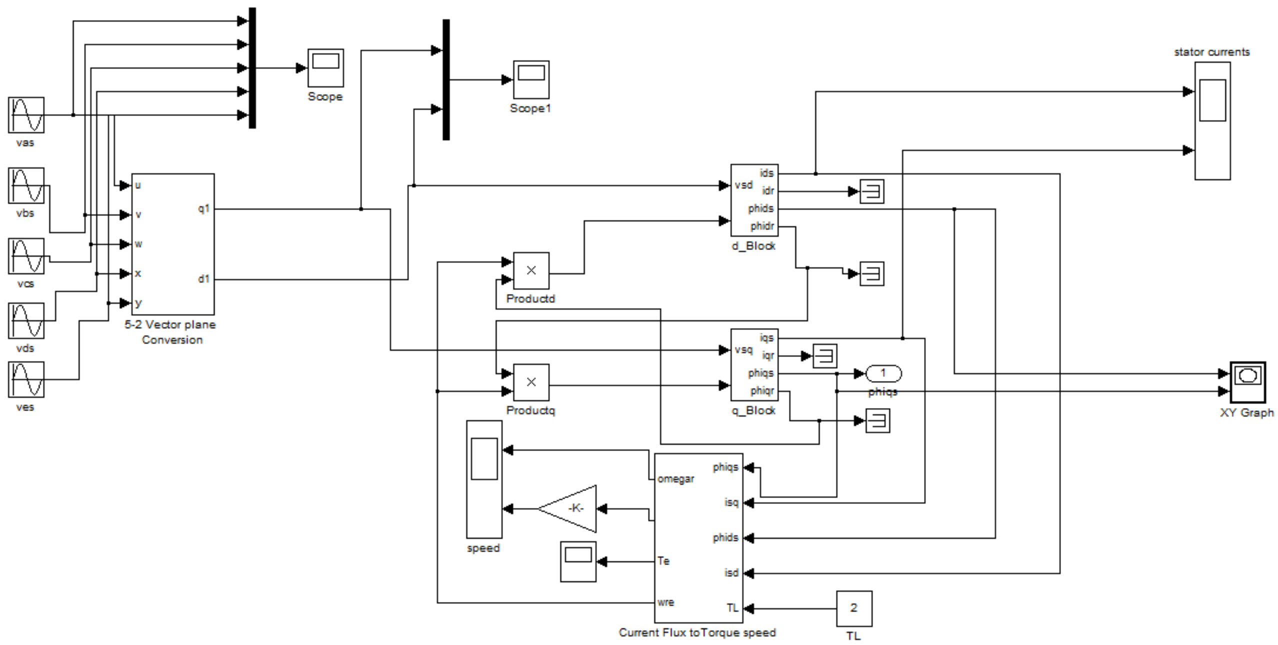

Fig.2.3.Simulation model of five-phase induction machine.

The parameters of the induction machine are given in Table-2.1. The *d-q* axes flux linkage blocks are modeled separately using the equations (2.20)-(2.23). The input voltage for the machine block is provided using two-phase *d-q* axis signal which is obtained from conversion of the five-phase input voltages as given in equation (2.19). Fig. 2.4 shows the *d-q* axes flux trajectory in steady state for the simulated induction machine. The flux trajectory is a circle indicating a balanced simulated machine fed from a balanced supply. The detailed description of the five-phase drive and control is explained in next chapter.

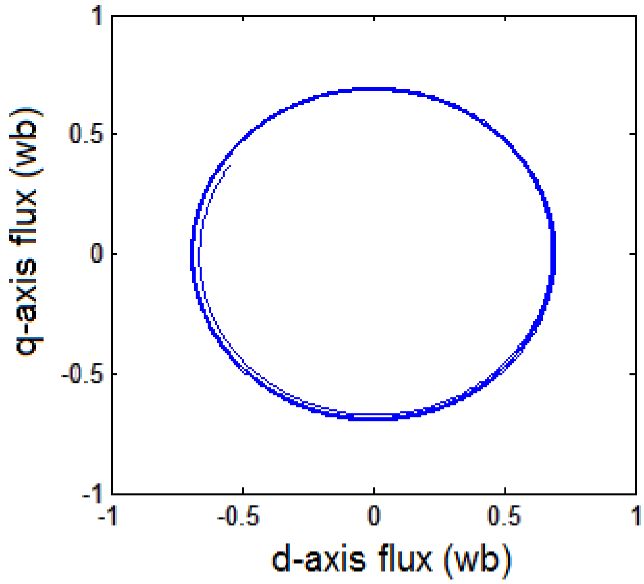

Fig. 2.4. *d-q* axes flux trajectory for the induction machine.

Table 2.1: Induction machine parameters

Power rating	1.5 kW
Voltage rating	400V, 50Hz
Stator poles	4
Stator resistance	6.03 Ω
Rotor resistance	6.085 Ω
Stator leakage inductance	0.039 mH
Rotor leakage inductance	0.039 mH
Magnetizing inductance	0.45 mH
Inertia constant	0.0158
Friction coefficient	0.00

CHAPTER 3

3. Speed control of five-phase induction motor using IFOC method

3.1 Introduction

The vector control can be implement either by direct method or indirect method. The methods can be distinguished by how the unit vectors (cosθ_e and sinθ_e) are generated for the control scheme. In direct control, flux vector are computed from terminal quantities of the motor, but in indirect control, motor slip frequency ω_{sl} is required to compute the desired flux vector. Fig. 3.1 (a) explains the fundamental principle of indirect vector control. The flow diagram for the same is shown in Fig.3.1 (b). The d^e-q^e axes are fixed on the stator and the d^r-q^r axes, which are fixed on the rotor, are moving at speed ω_r as shown. Synchronously rotating axes d^e-q^e are rotating ahead of the d^r-q^r axes by the positive slip angle θ_{sl} corresponding slip frequency ω_{sl}. Since the rotor pole is directed on the d^e axis, thus $\omega_e = \omega_r + \omega_{sl}$. θ_e is expressed as,

$$\theta_e = \int (\omega_r + \omega_{sl}) \mathrm{dt} = \theta_r + \theta_{sl} \tag{3.1}$$

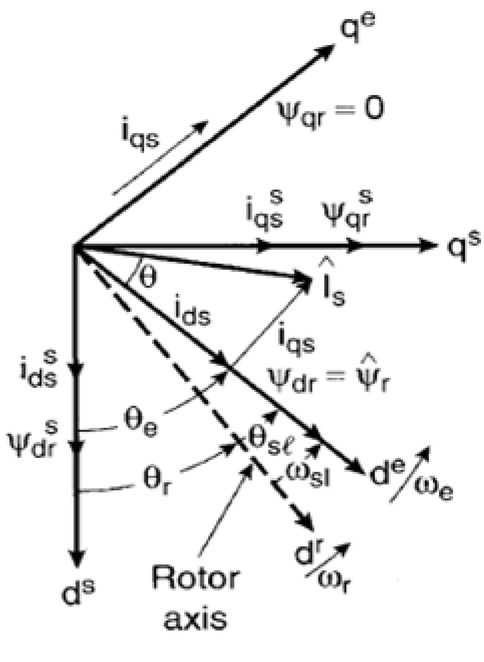

(a)

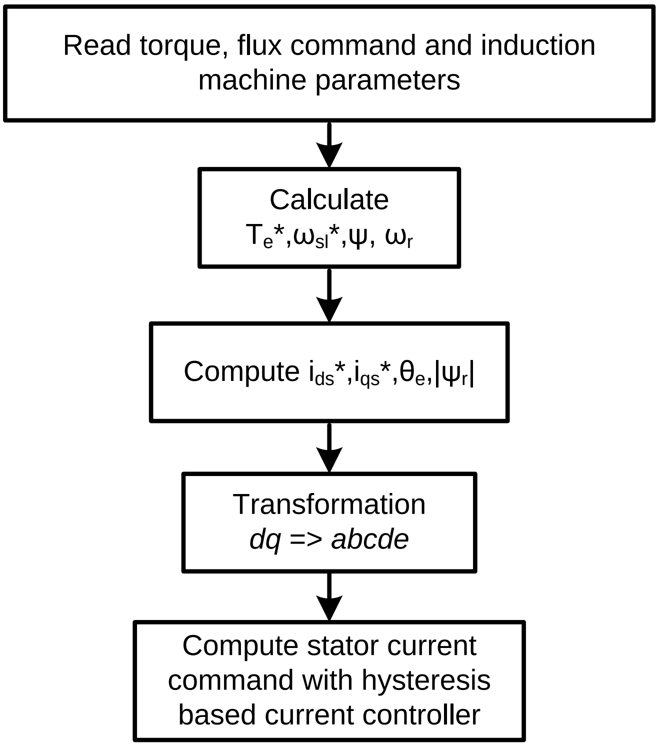

(b)

Fig.3.1. (a) Phasor diagram: Indirect Vector Control (b) Process flow diagram for Indirect Vector Control.

The phasor diagram Fig.3.1.(a) suggests that for decoupling control, the stator flux component of current i_{ds} should be aligned on the d^e axis and the torque component of current i_{qs} should be on the q^e axis.

3.2 IFOC based speed control

For decoupling control in d^e-q^e frame, the rotor circuit equations can be written as,

$$0 = R_s i_{dr} + p\psi_{dr} + (\omega_e - \omega_r)\psi_{qr} \tag{3.2}$$

$$0 = R_s i_{qr} + p\psi_{qr} - (\omega_e - \omega_r)\psi_{dr} \tag{3.3}$$

The rotor flux linkage equations are,

$$\begin{aligned} \psi_{dr} &= L_r i_{dr} + L_m i_{ds} \\ \psi_{qr} &= L_r i_{qr} + L_m i_{qs} \end{aligned} \tag{3.4}$$

From the above equation, expressing d-axis rotor current in terms of q-axis stator current and corresponding rotor flux,

$$
\begin{aligned}
i_{dr} &= \frac{1}{L_r}\psi_{dr} + \frac{L_m}{L_r} i_{ds} \\
i_{qr} &= \frac{1}{L_r}\psi_{qr} + \frac{L_m}{L_r} i_{qs}
\end{aligned}
\tag{3.5}
$$

Replacing i_{dr} and i_{qr} from (3.5) in (3.2) and (3.3),

$$p\psi_{dr} + \frac{R_r}{L_r}\psi_{dr} - \frac{L_m}{L_r} R_s i_{ds} - \omega_{sl}\psi_{qr} = 0 \tag{3.6}$$

$$p\psi_{qr} + \frac{R_r}{L_r}\psi_{qr} - \frac{L_m}{L_r} R_s i_{qs} - \omega_{sl}\psi_{dr} = 0 \tag{3.7}$$

For decoupling control, the total rotor flux is aligned to d-axis. Thus, $\psi_{qr} = 0$ and thus, $p\psi_{qr} = 0$.

Also, $\psi_{dr} = \psi_r$. Replacing these conditions in equations (3.6) and (3.7),

$$\frac{L_r}{R_r} p\psi_r + \frac{R_r}{L_r}\psi_r = L_m i_{ds} \tag{3.8}$$

$$\omega_{sl} = \frac{L_r R_r}{\psi_r L_r} i_{qs} \tag{3.9}$$

If rotor flux is constant, from (3.8),

$$\psi_r = L_m i_{ds} \tag{3.10}$$

$$i_{ds} = \frac{\psi_r}{L_m} \tag{3.11}$$

From the torque equation of five-phase motor, i_{qs} can be expressed as,

$$i_{qs} = \frac{2}{5}\left(\frac{2}{P}\right)\frac{L_m T_e}{L_r \psi_r} \tag{3.12}$$

Comparing equation (3.1) and (3.9),

$$\theta_e = \int \left(\omega_r + \left(\frac{L_m i_{qs}}{T_r \psi_r} \right) \right) \mathrm{dt} \tag{3.13}$$

Where, $T_r = \frac{L_r}{R_r}$.

Considering the equations (3.1), (3.9), (3.11)-(3.13), the indirect vector control model is implemented in Fig 3.2 [3],[5]-[6]. In this diagram, the induction motor is fed by a current-controlled PWM inverter, which operates as a three-phase sinusoidal current source. The d^e-axis control is responsible for maintaining the rotor flux at rated value while the q^e-axis control is responsible for controlling the torque. Control of both these quantities can be achieved by using proportional-integral (PI) controllers since the signals in d^e-q^e reference frame are typically steady DC quantities. The motor speed ω_r is compared to the reference ω_r* and the error is processed by the speed controller to produce a torque command T_e*. The stator quadrature-axis current reference i_{qs}* is calculated using the torque reference T_e* as in equation (3.12). The stator direct-axis current reference i_{ds}* is obtained from rotor flux reference input $|\psi_r|$* in equation (3.11). The rotor flux position θ_e required for coordinates transformation is generated from the rotor speed ω_r and slip frequency ω_{sl}. The slip frequency is calculated from the stator reference current i_{qs}* and the motor parameters in equation (3.13). The i_{qs}* and i_{ds}* current references are converted into phase current references I_c* (phases- *a-b-c-d-e*) for the current regulators. The regulators process the measured and reference currents to produce the inverter gating signals.

The role of the speed controller is to keep the motor speed follow to the speed reference input in steady state and to provide a good dynamic response during transients. The controller used here is a PI type as already mentioned due to its obvious advantages.

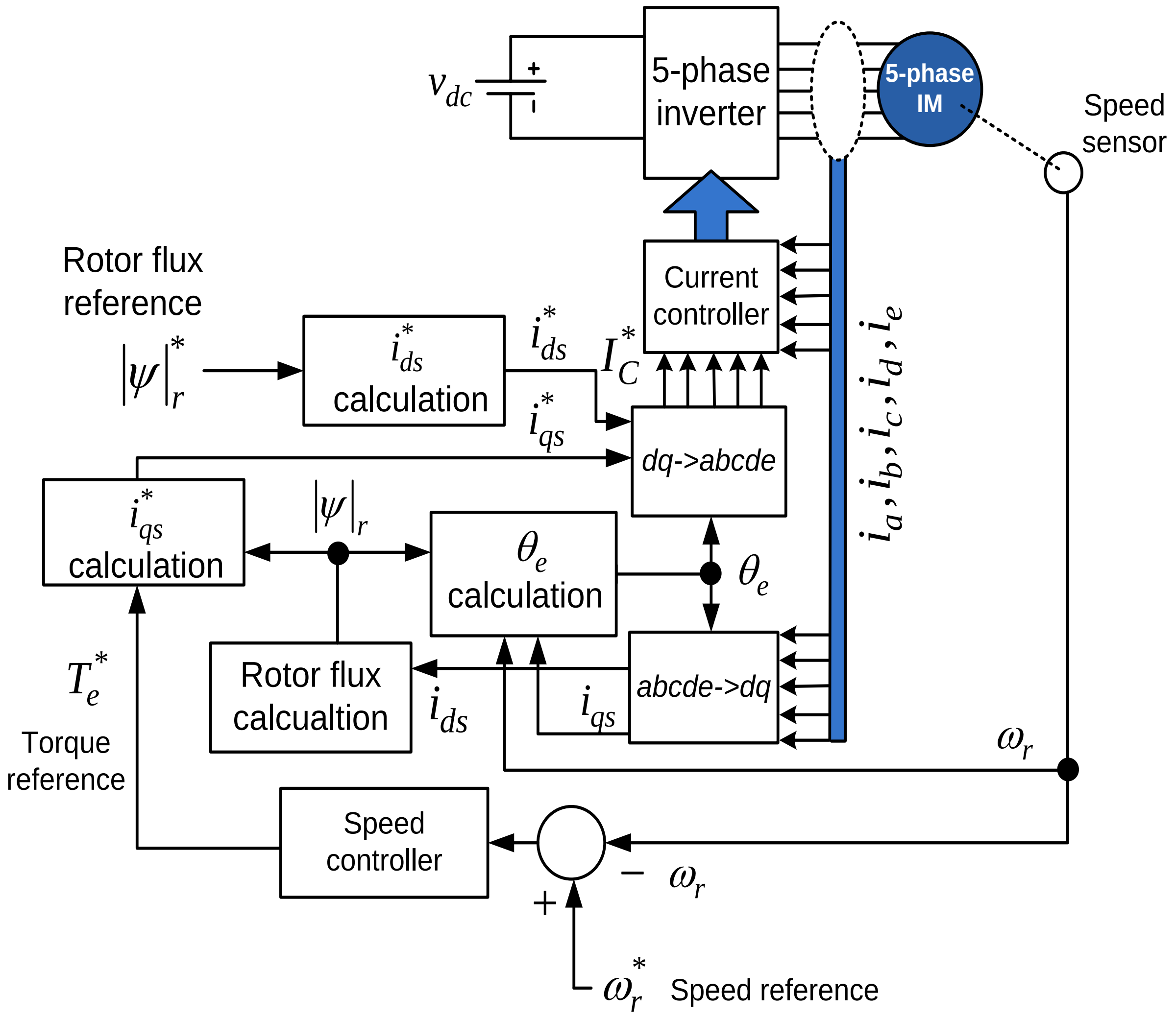

Fig.3.2. Block diagram of indirect vector control of five-phase induction motor.

For the simulated five-phase induction machine, the parameters considered for the equations (3.1), (3.9), (3.11)-(3.13) are,

$$i_{ds} = 2.22\psi_r \tag{3.14}$$

$$i_{qs} = 0.3622\frac{T_e}{\psi_r} \tag{3.15}$$

$$\omega_{sl} = 5.6\frac{i_{qs}}{\psi_r} \tag{3.16}$$

$$T_r = 0.080419 \tag{3.17}$$

CHAPTER 4

4. Simulation Results

4.1 Introduction

Induction motors and their drives have been an active area of research due to their ruggedness and longevity. Advances in power electronic devices have enabled implementation of new control topologies besides upgrading the existing ones. To estimate and verify and validate the performance of five-phase induction machine and to study the performance of its control strategy, a simulation study is performed in *MATLAB/Simulink R2012b,* a simulation tool developed by 'The Mathworks Inc.'. MATLAB is chosen for the simulation study as it is inherently advantageous as regards ease of implementation in block diagram form, availability of good solver modules, ease of calculations and easier interface. The system can also be effectively close loop controlled using different available toolboxes.

4.2 Simulation of a five-phase inverter

For driving the five-phase induction machine, a five-phase inverter system is used. The five-phase inverter is built in *Simulink* platform using the *Simulink* and *SimPowerSystem* toolboxes. IGBT devices are used for this purpose. The model of IGBT available in *SimPowerSystem* toolbox is used with internal resistance of 1e-3 and snubber resistance and capacitance of 1e5 and infinity.

The induction machine stator coils when excited by balanced five-phase sinusoidal supply produces a rotating magnetic field of constant magnitude. The revolving field interacts with rotor to produce useful torque. It is difficult to obtain pure sinusoidal voltages from static inverters. The inverter output voltage will contain time harmonics which will inject harmonic currents into the machine stator. The five-phase connection effectively eliminates the fifth- and other quintuple-order harmonics. However, the other harmonics will be present with varying magnitudes and phase sequences. The topology of a five-phase inverter with a five-phase motor is shown in Fig.4.1.

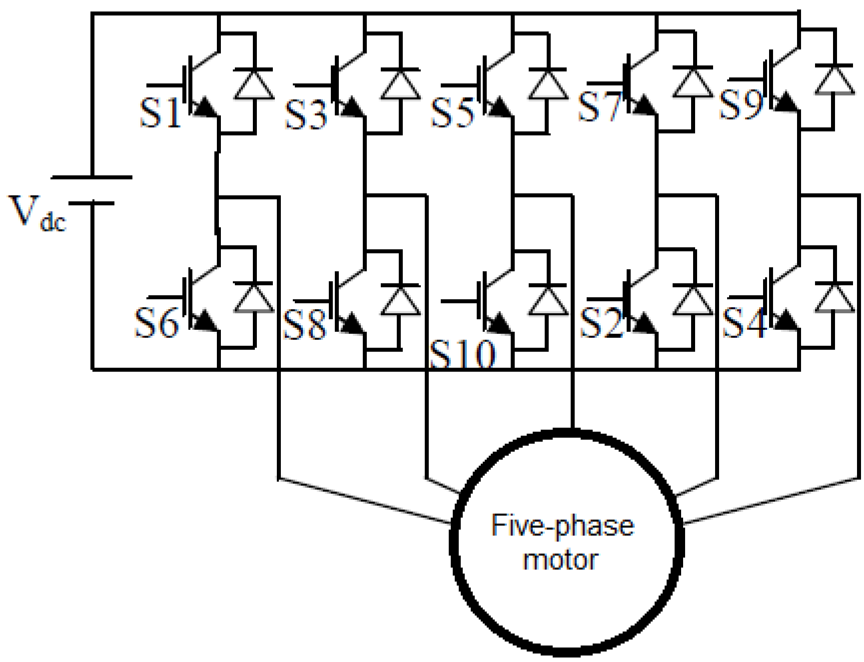

Fig.4.1. Five-phase inverter driving a five-phase motor.

The simulation diagram of the five-phase inverter is shown in Fig.4.2 below.

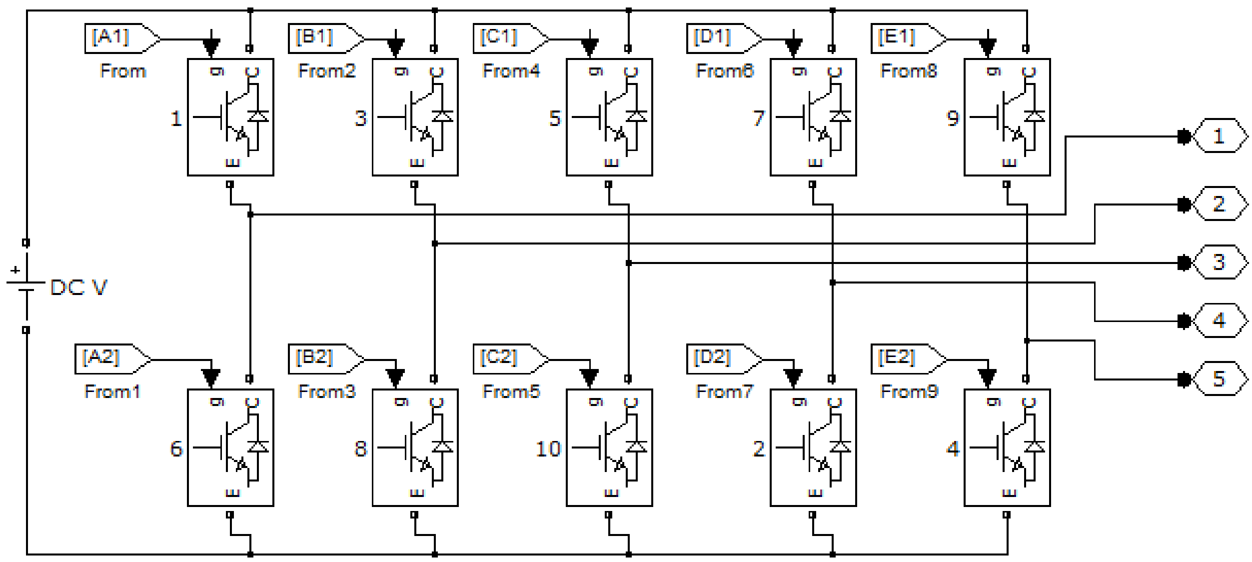

Fig.4.2. Simulation diagram for five-phase inverter.

In this inverter, generally, three switches from the upper limb and two from the lower switches are turned on at a time during positive half and vice versa during negative half of a full cycle. The switching sequence and the mode of operation of a five-phase inverter are shown below in Fig.4.3.

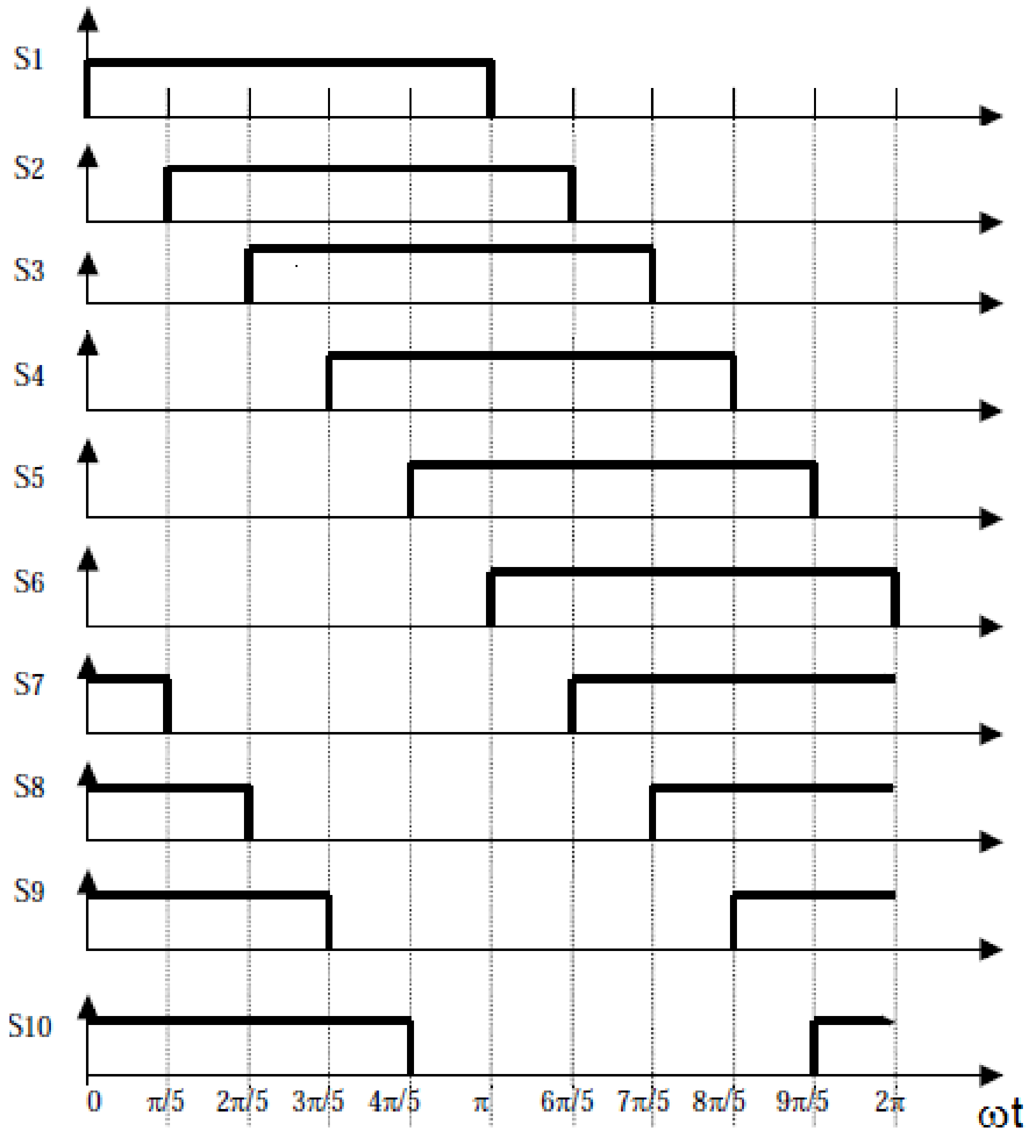

Fig.4.3. Switching sequence of five-phase inverter.

Table 4.1 shows the switching states of the individual switches pertaining to Fig.4.3.

Sinusoidal pulse width modulation (SPWM) based switching technique is used to generate the pulses for the IGBTs. In this technique, a triangular carrier wave is compared with the sine wave to generate the pulses.

Table 4.1: Switching states of the individual switches pertaining to Fig.4.3

MODE	SWITCHES 'ON'															TERMINAL POLARITY				
9	1	7	8	9	10											A^+	B^-	C^-	D^+	E^-
10			8	9	10	1	2									A^+	B^-	C^-	D^-	E^+
1				9	10	1	2	3								A^+	B^+	C^-	D^-	E^+
2					10	1	2	3	4							A^+	B^+	C^-	D^-	E^-
3						1	2	3	4	5						A^+	B^+	C^+	D^-	E^-
4							2	3	4	5	6					A^-	B^+	C^+	D^-	E^-
5								3	4	5	6	7				A^-	B^+	C^+	D^+	E^-
6									4	5	6	7	8			A^-	B^-	C^+	D^+	E^-
7										5	6	7	8	9		A^-	B^-	C^+	D^+	E^+
8											6	7	8	9	10	A^-	B^-	C^-	D^+	E^+

The output line-line voltages from the five-phase inverter are shown in Fig. 4.4. The five-phase voltage and its filtered form when passed through a low pass filter of cut off frequency 200Hz and damping factor of 0.707 is shown in Fig. 4.5 (a) and Fig.4.5 (b) respectively.

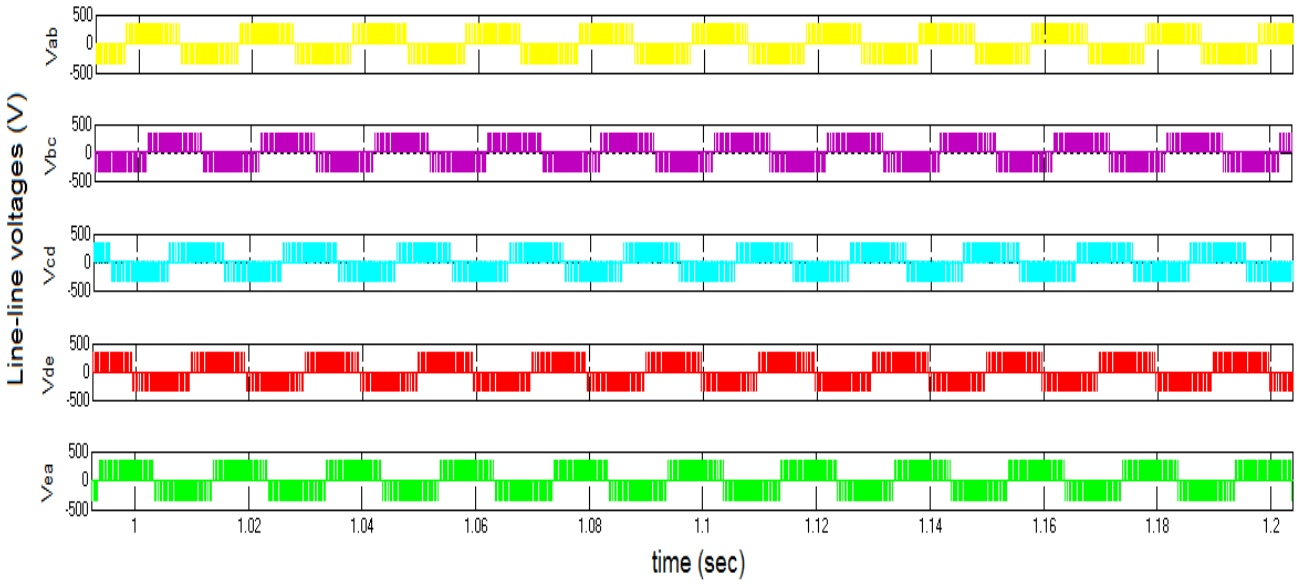

Fig.4.4. Line-line voltages for the inverter.

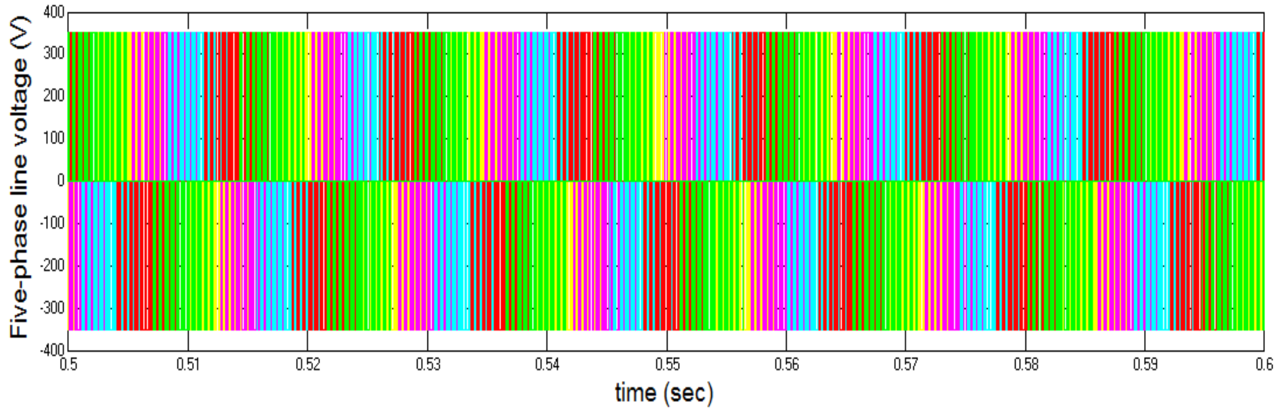

(a)

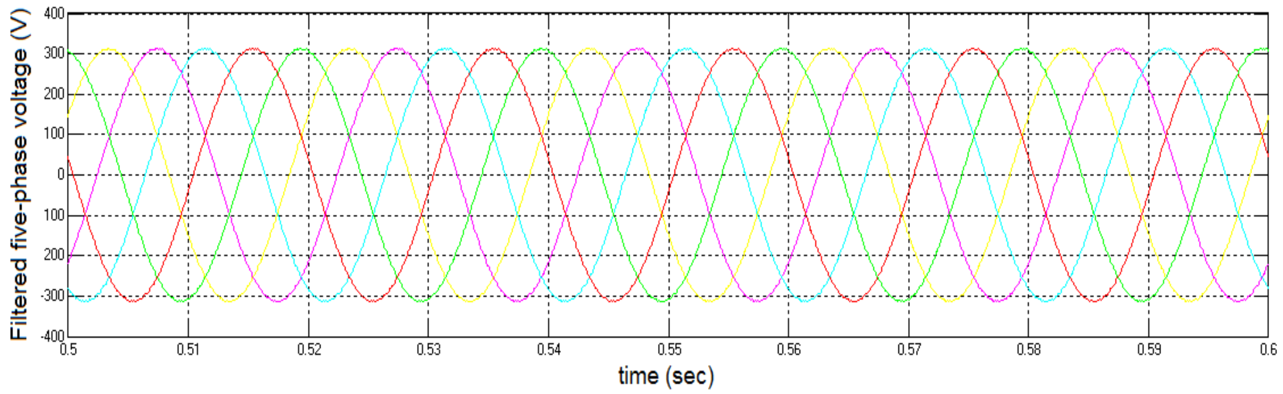

(b)

Fig.4.5. (a) Five-phase voltage output from the PWM inverter (b) filtered voltage output for the same.

4.3 Simulation of inverter fed five-phase induction motor drive

The five-phase induction motor model is briefly presented in Section 2.3. In the simulation model, stationary d^s-q^s axes equations (2.20)-(2.25) and (1.14)-(1.17) are used. The internal model is based on the flux equations and the flux to torque speed equations. The same is shown in Fig.4.6 (a), (b) and (c) respectively.

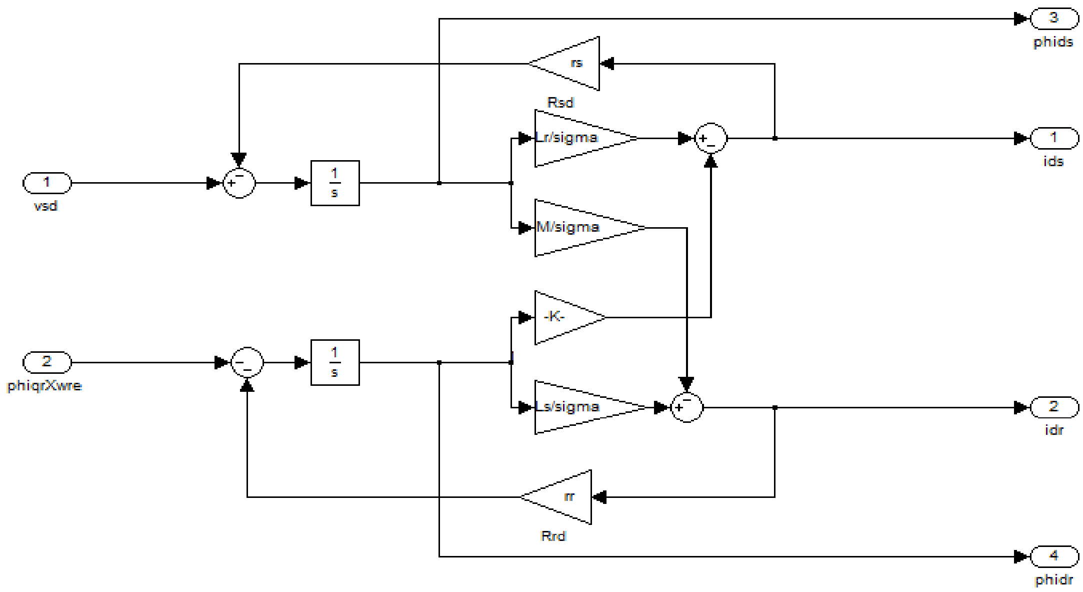

3
phids
rs
Rsd
Lr/sigma
1
ids
1
vsd
1
s
M/sigma
-K-
2
phiqrXwre
1
s
Ls/sigma
2
idr
rr
Rrd
4
phidr

(a)

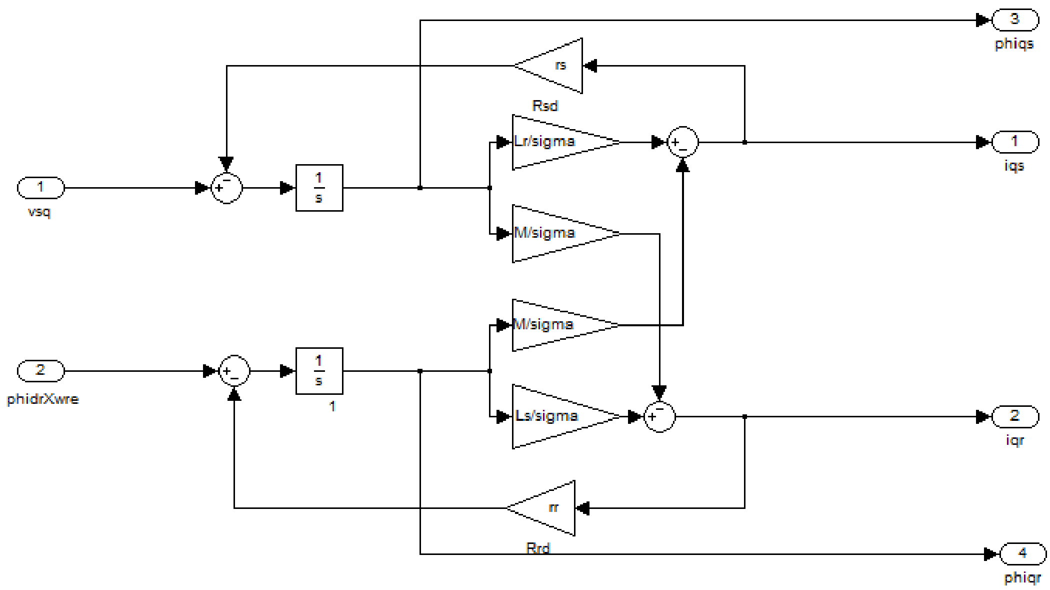

3
phiqs
rs
Rsd
Lr/sigma
1
iqs
1
vsq
1
s
M/sigma
M/sigma
2
phidrXwre
1
s
1
Ls/sigma
2
iqr
rr
Rrd
4
phiqr

(b)

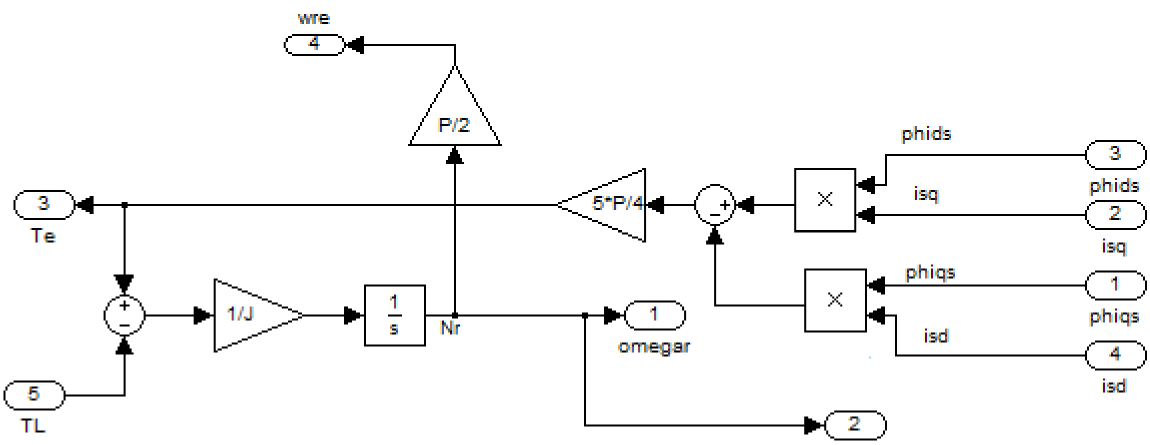

(c)

Fig.4.6. (a) d^s-axis flux model (b) q^s-axis flux model and (c) flux-torque-speed model.

The d^s-q^s axes flux linkage and voltage equations are represented in Fig.4.6 (a) and Fig.4.6 (b) respectively. The Fig.4.6 (c) represents the torque equation and the speed output from the motor. Thus it can also be regarded as the machine mechanical model as given in (2.24)-(2.25). The overall model of the inverter fed five-phase induction machine model is shown in Fig.4.7.

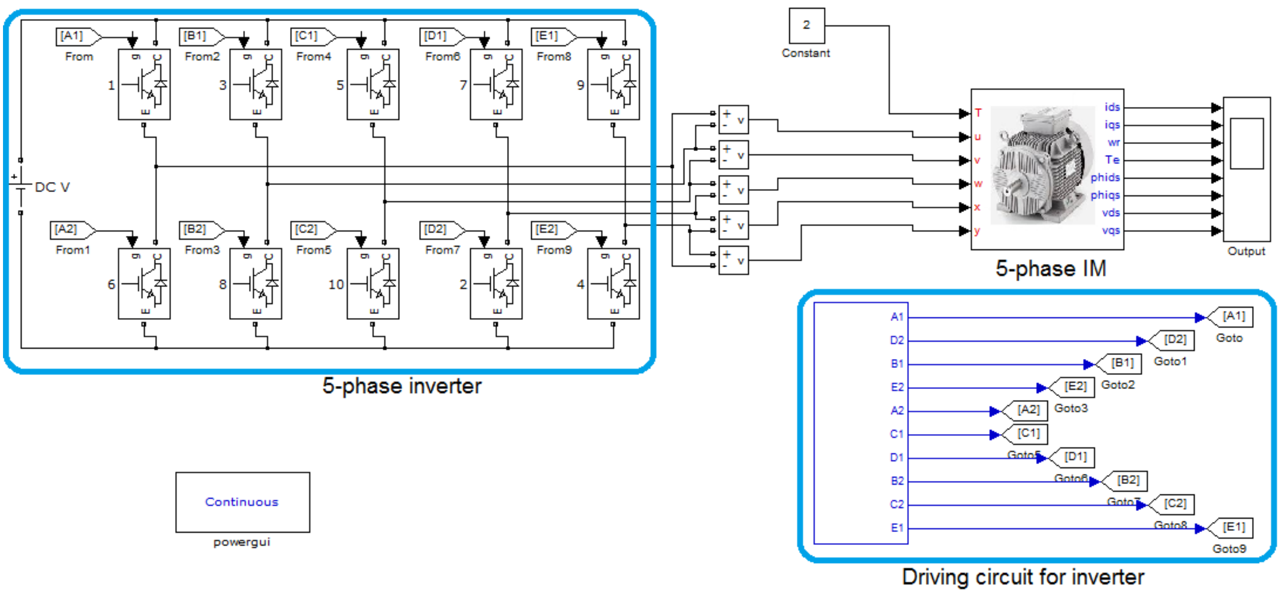

Fig.4.7. Open-loop five-phase inverter fed five-phase induction motor drive system.

The steady state waveforms for the inverter fed five-phase induction machine is shown next in the thesis. Fig.4.8 (a) shows the stator *d-q* axes currents when the PWM inverter-fed open-loop induction machine of Fig.4.7 is loaded with a torque of 2 N-m. Fig.4.8 (b) shows the corresponding stator fluxes.

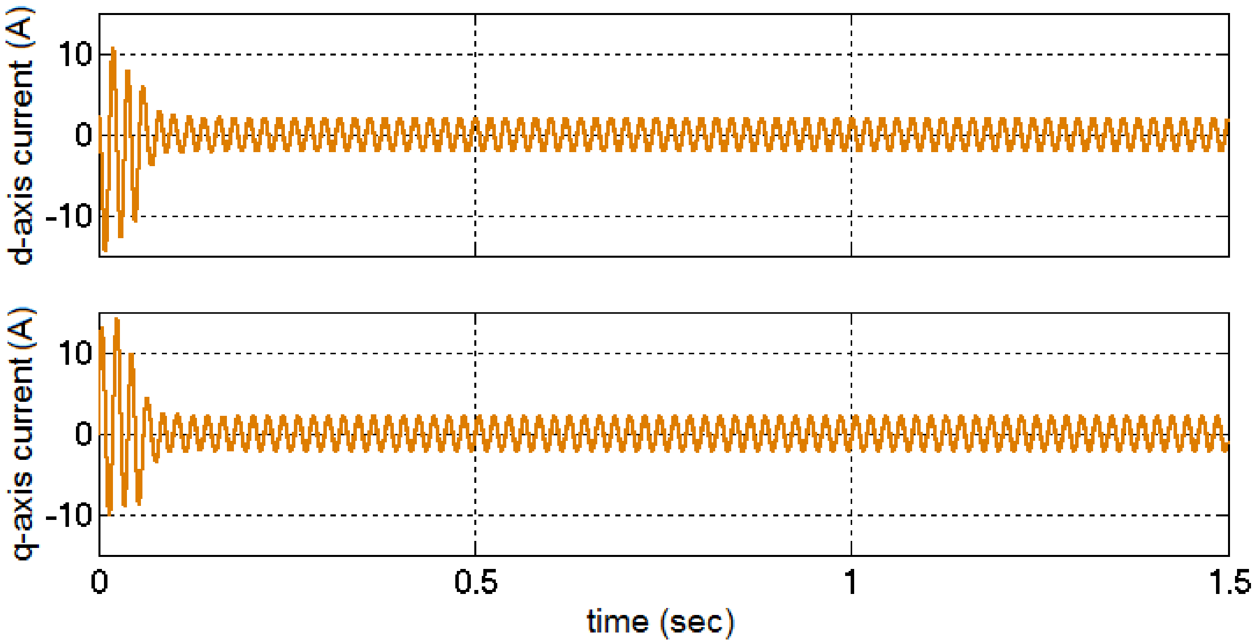

(a)

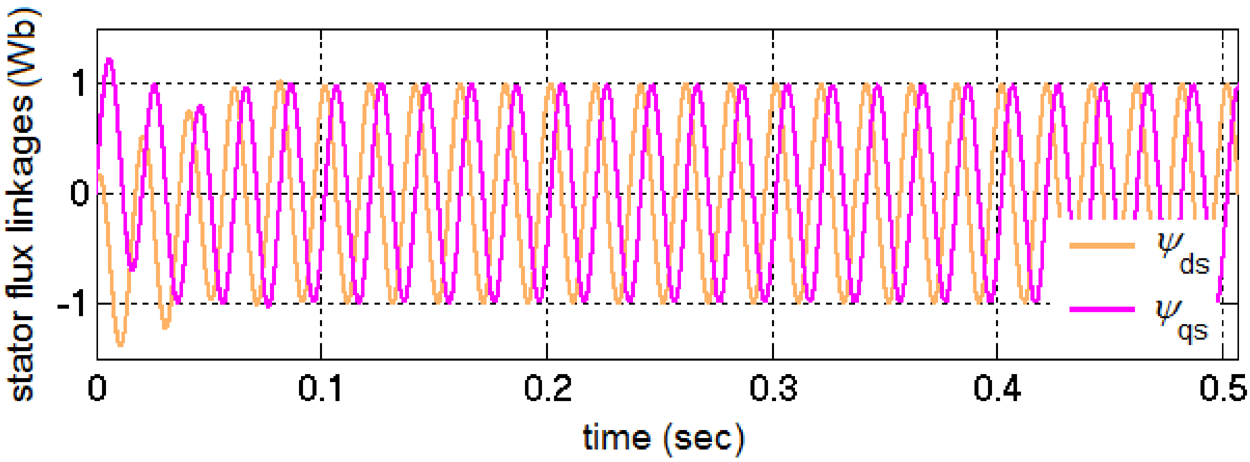

(b)

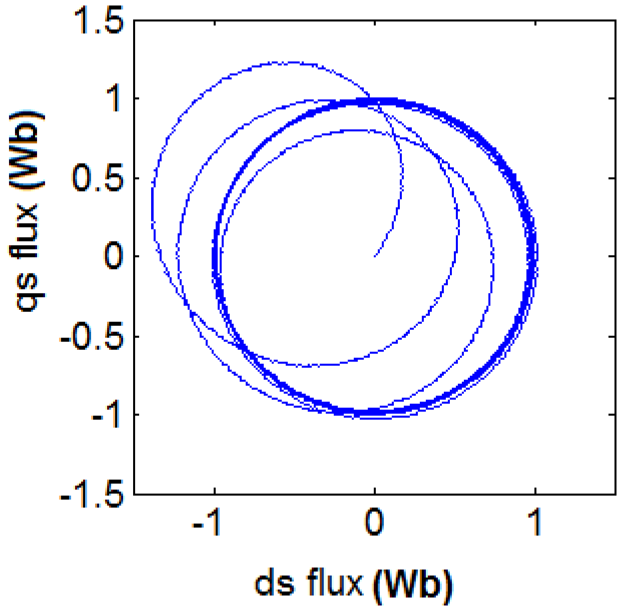

(c)

Fig.4.8. Five-phase induction machine d^s-q^s axes (a) stator currents (b) stator fluxes and (c) flux trajectory.

As observed from the induction machine sinusoidal stator currents and flux linkages, the machine is balanced and gives good transient and steady state performance. The same is verified from the stator flux linkage trajectory of Fig.4.8 (c). The induction machine speed and torque waveforms are shown in Fig. 4.9 (a) and Fig.4.9 (b) respectively.

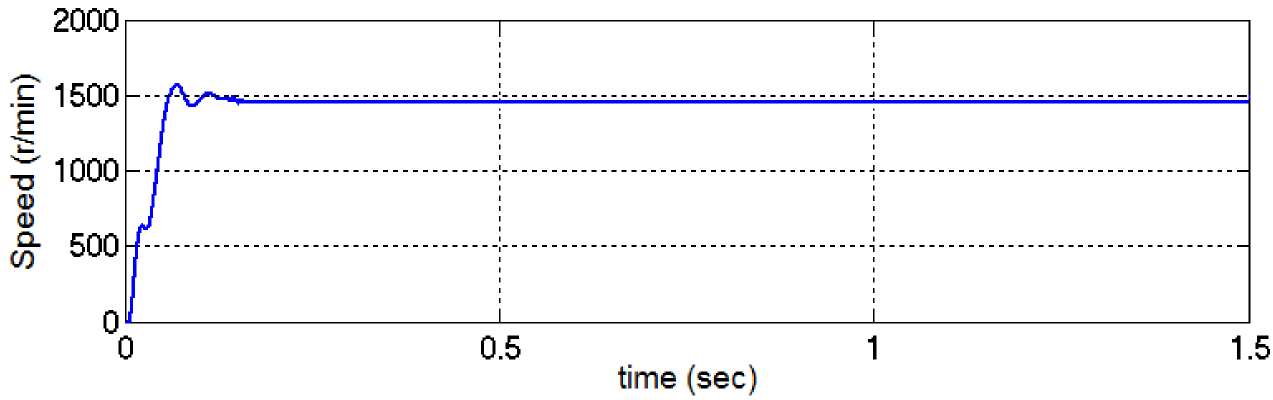

(a)

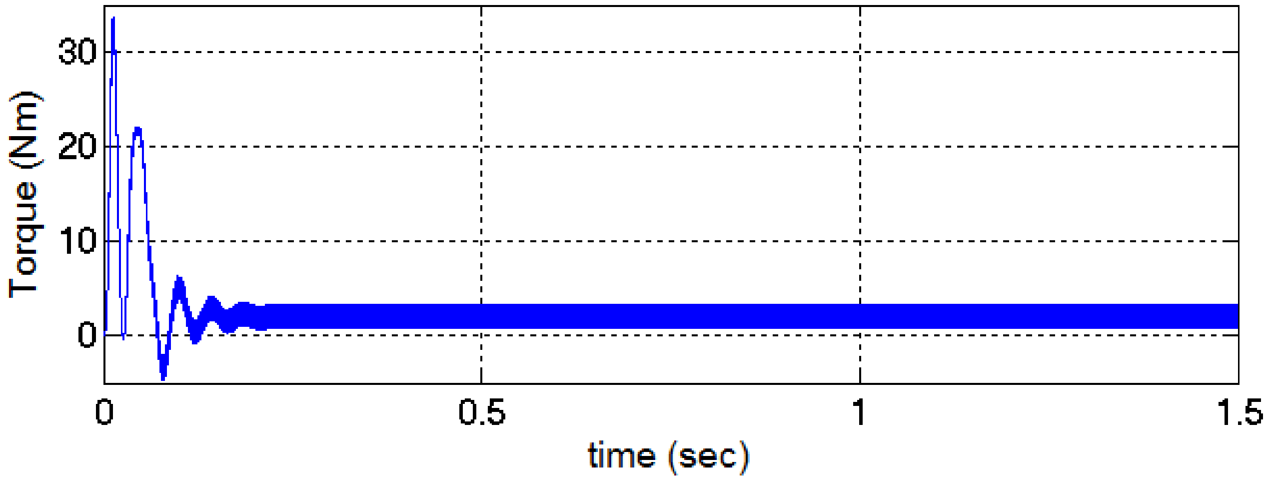

(b)

Fig.4.9. Five-phase induction machine (a) speed and (b) electromagnetic torque (T_L = 2 Nm).

The induction motor exhibits a steady speed of 1480 r/min as it reaches the steady state as observed from Fig.4.9 (a). Also as observed from Fig.4.9 (b), at steady state, the electromagnetic torque matches the load torque. The torque waveform is observed to be having steady pulsations of about 0.25 Nm and it is attributed to some minor unbalance in the stator currents caused due to some error in calculation of the machine parameters.

4.4 Simulation of IFOC based five-phase induction motor drive

For the closed loop speed control of the five-phase induction motor, IFOC based control is proposed in this thesis. The block diagram of the proposed control scheme is shown in Fig.3.2. In this scheme, the control structure has been obtained from the dynamic model of five-phase induction motor drive system using the vector control technique. The effectiveness of the control has been ascertained by performance prediction of a *MATLAB* based simulation of five-phase induction motor drive over a wide range of operating conditions. The *Simulink* block diagram of the proposed control scheme is shown in Fig.4.10.

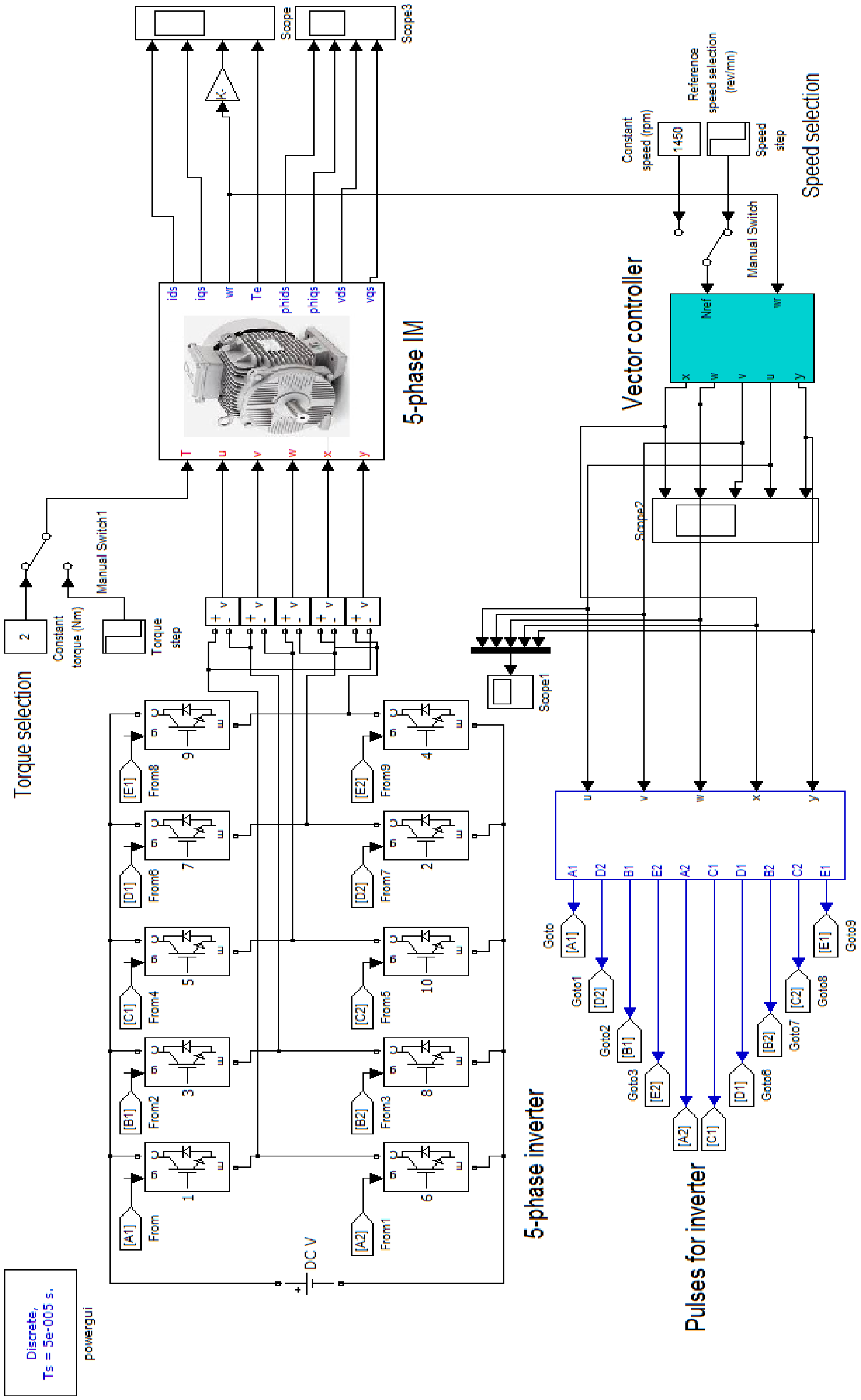

Fig.4.10. Five-phase induction machine IFOC model in *MATLAB/Simulink*.

The controller is implemented in *Simulink* using the (3.1), (3.9), (3.11)-(3.13) with the parameters used from (3.14)-(3.17). The controller block in *Simulink* is shown in Fig.4.11.

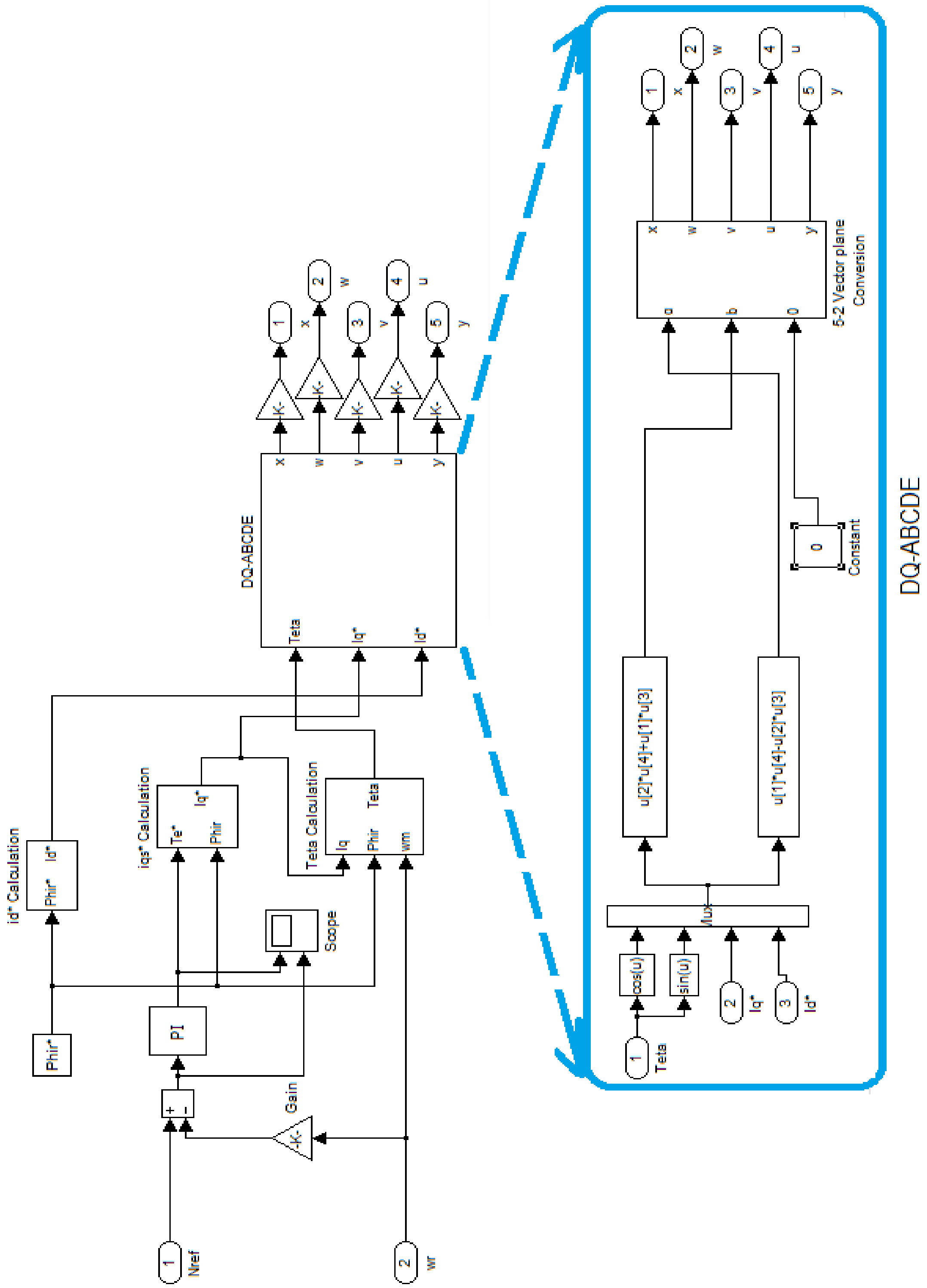

Fig.4.11. Five-phase induction machine IFOC controller model in *MATLAB/Simulink*.

4.4.1 Description of the controller

The proposed control system block is shown in Fig.4.11. In the control block, the reference stator currents i_{ds}* and i_{qs}* are generated using equations (3.11) and (3.12) respectively. The equations use the machine parameters as given in Table 2.1. After calculations, the equations (3.14)-(3.15) are used to simulate the model stator reference currents. Similarly, for finding the θ_e, equation (3.13) is used where the value of T_r is taken from equation (3.17) obtained by putting the machine circuit parameters. The value of ω_{sl} is calculated from equation (3.9) and the final equation obtained which is used for θ_e calculation is equation (3.16).

Finally, the obtained i_{ds}*, i_{qs}* and θ_e are used to calculate the *as-bs-cs-ds-es* currents after converting the former into αs-βs axes reference stator currents as,

$$\begin{bmatrix} i_{\alpha s}^* \\ i_{\beta s}^* \end{bmatrix} = \begin{bmatrix} \sin\theta_e & -\cos\theta_e \\ \cos\theta_e & \sin\theta_e \end{bmatrix} \begin{bmatrix} i_{ds}^* \\ i_{qs}^* \end{bmatrix} \tag{4.1}$$

Where, * denotes reference quantities. Equation (4.1) is then converted back to *as-bs-cs-ds-es* currents using inverse of equation (2.19). The obtained *as-bs-cs-ds-es* reference stator currents are then compared with actual *as-bs-cs-ds-es* currents in a hysteresis band based current controller to generate the pulses for driving the inverter.

4.4.2 Variation of speed and torque references

The induction motor controller can work with varying speed and torque set references. For this purpose, provision is kept to externally vary the speed and load torque input to the five-phase induction machine. This is achieved with the proposed control and is implemented in the simulation model using the manual switch as shown in the Fig.4.10. The speed reference and the actual speed of the machine are compared and fed to a proportional-integral (PI) based controller for generating the theta as shown in Fig.4.11.

4.5 Simulation Results

The IFOC based control of the five-phase induction machine is simulated using discrete time sampling with sample time of 50e-6 seconds. The machine is run with a steady load torque (T_L) of 2 Nm. The reference speed is set at 1450 r/min. The simulated stator currents, speed and torque response are shown in Fig.4.12 (a) and stator fluxes Fig.4.12 (b) respectively.

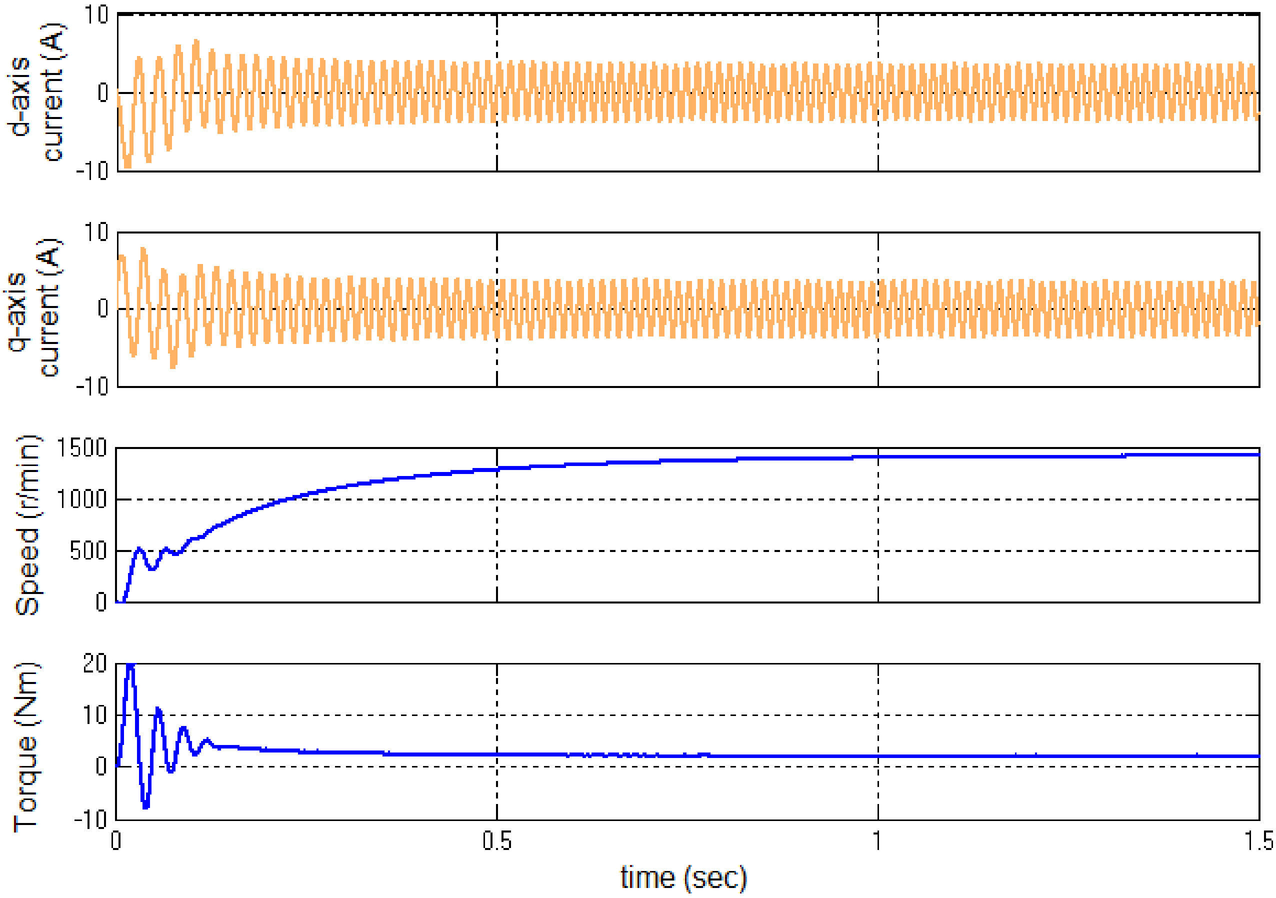

(a)

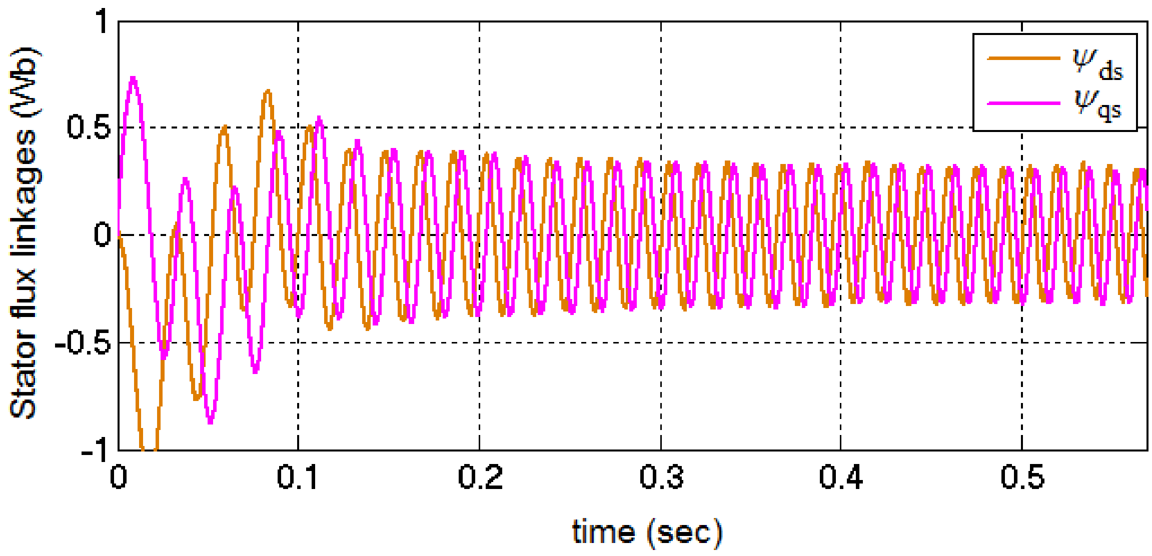

(b)

Fig.4.12. Five-phase induction machine IFOC waveforms for (a) stator currents, speed and torque response (b) stator flux linkages in d^s-q^s frame.

The stator flux trajectory is shown in Fig.4.13 below.

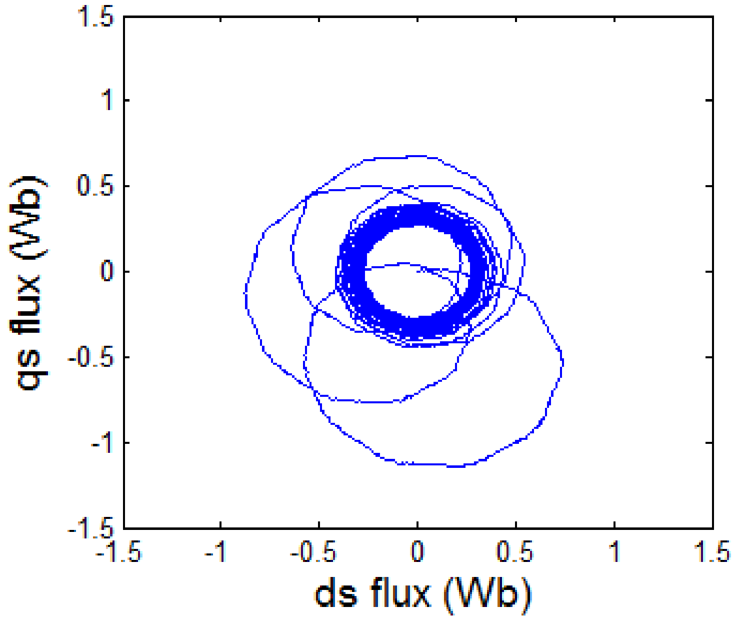

Fig.4.13. Five-phase induction machine stator d^s-q^s axis flux trajectory with IFOC.

Next, the dynamic response of the IFOC is checked by keeping the torque reference same at 2 Nm and varying the reference speed first from 1400 r/min to 800 r/min and again from 800 r/min to

1400 r/min as shown in Fig.4.14 (a) and Fig.4.14 (b) respectively. The change in speed is brought about at t = 2 sec and t = 1.5 sec respectively.

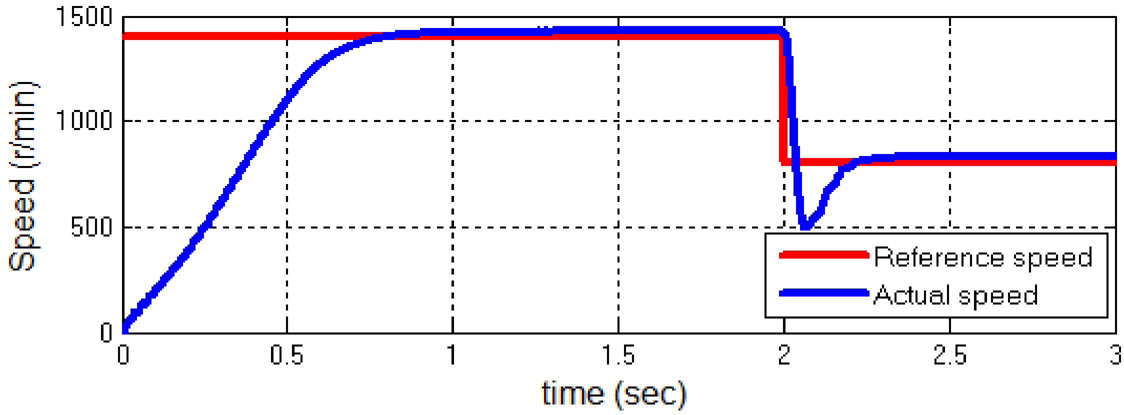

(a)

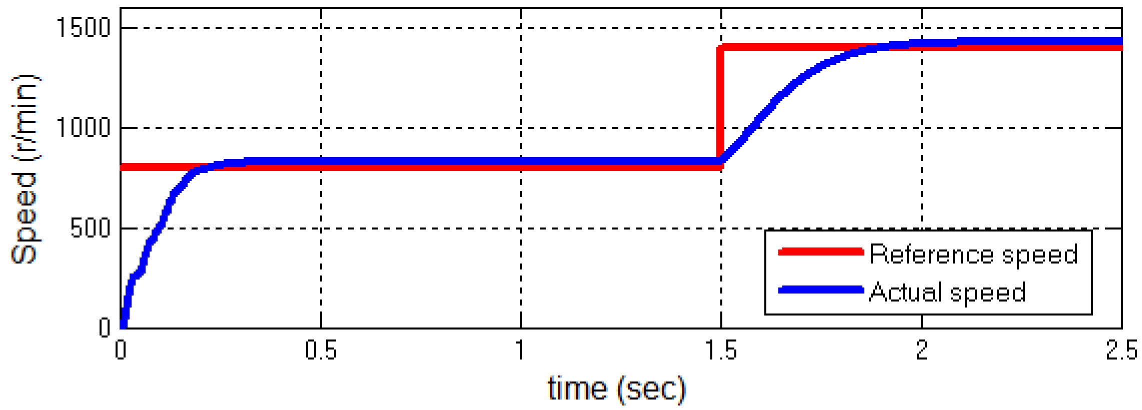

(b)

Fig.4.14. Variation of speed for the induction motor (a) step decrease from 1400 r/min to 800 r/min (b) step increase from 800 r/min to 1400 r/min.

For decrease in reference speed, the corresponding waveforms of the stator currents and torque are shown in Fig.4.15 (a) and flux trajectory in Fig.4.15 (b) respectively. As observed from the figures, the control scheme is shown to be giving good dynamic response. Similarly for increase in speed, the corresponding waveforms of the stator currents and torque are shown in Fig.4.15 (c) and flux trajectory in Fig.4.15 (d) respectively.

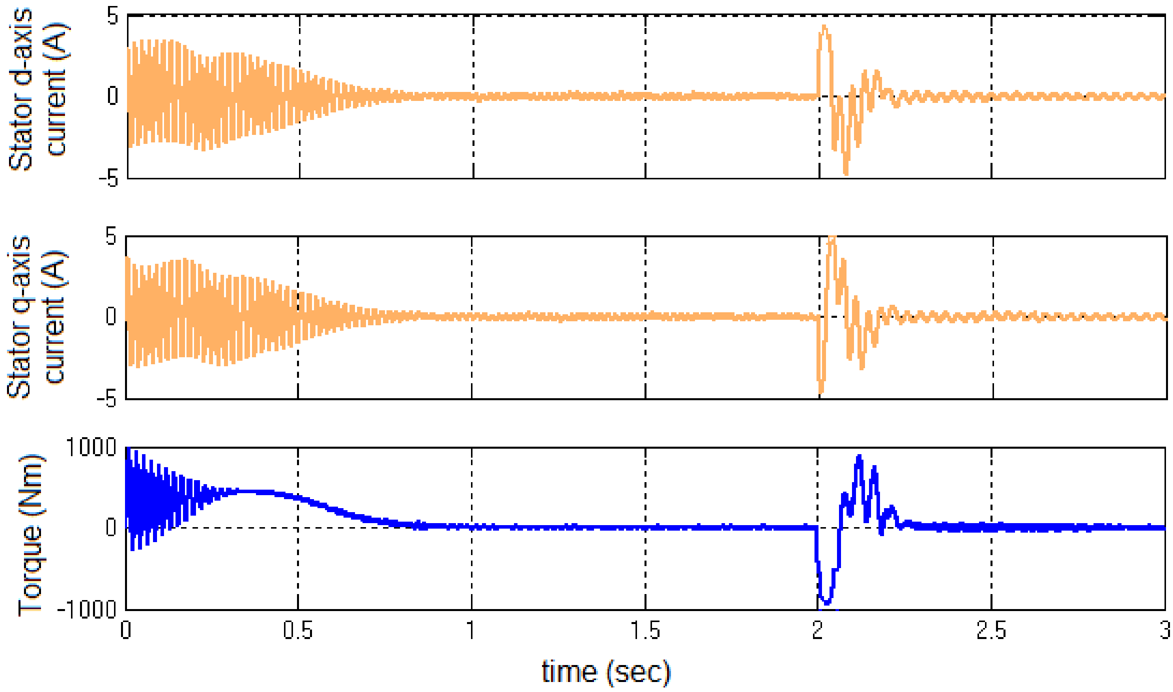
Stator d-axis current (A)
Stator q-axis current (A)
Torque (Nm)
time (sec)

(a)

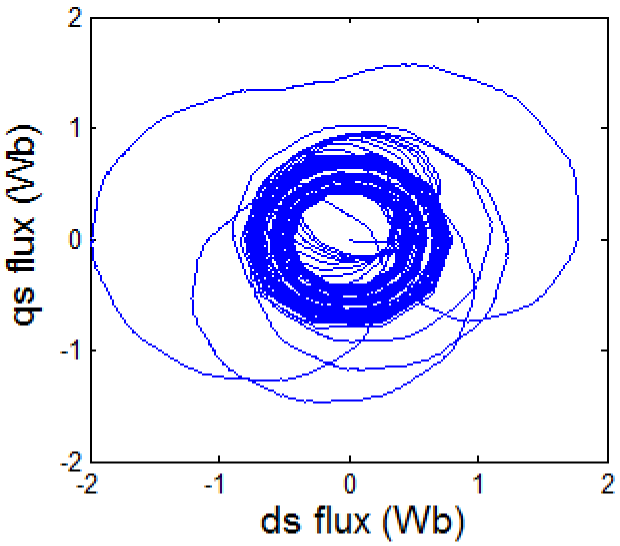
qs flux (Wb)
ds flux (Wb)

(b)

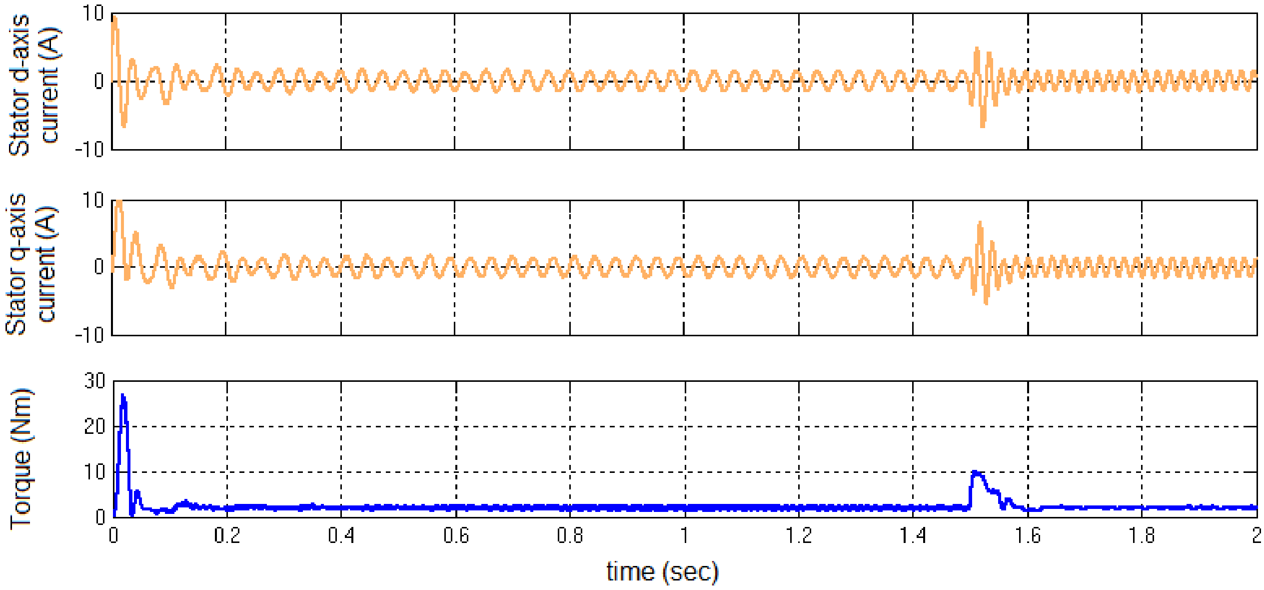

(c)

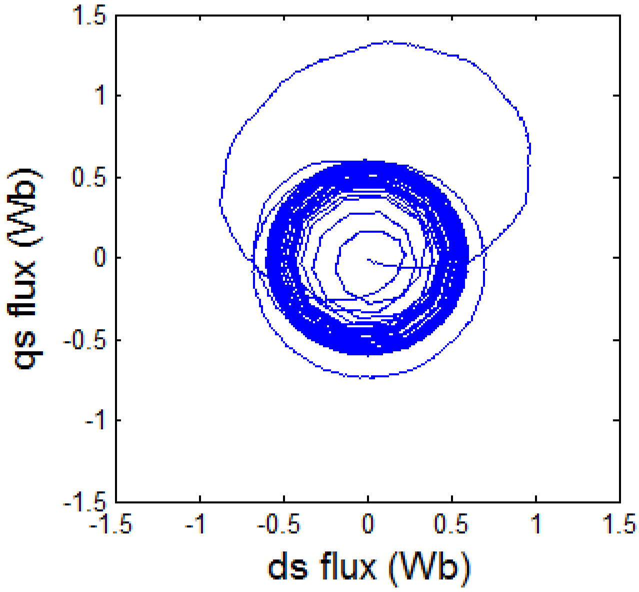

(d)

Fig.4.15. (a) stator currents and the torque with IFOC at constant load and varying speed from 1400 r/min to 800 r/min (b) flux trajectory for the same (c) stator currents and the torque with IFOC at constant load and varying speed from 800 r/min to 1400 r/min (d) flux trajectory for the same.

The dynamic response of the drive with changing torque reference is studied next. The torque reference is varied from 0 Nm to 3 Nm keeping the motor speed reference constant at 1450 r/min as shown in Fig.4.16. The plots for stator currents, speed and stator flux trajectory are as shown in Fig.4.17 (a) and Fig.4.17 (b) respectively.

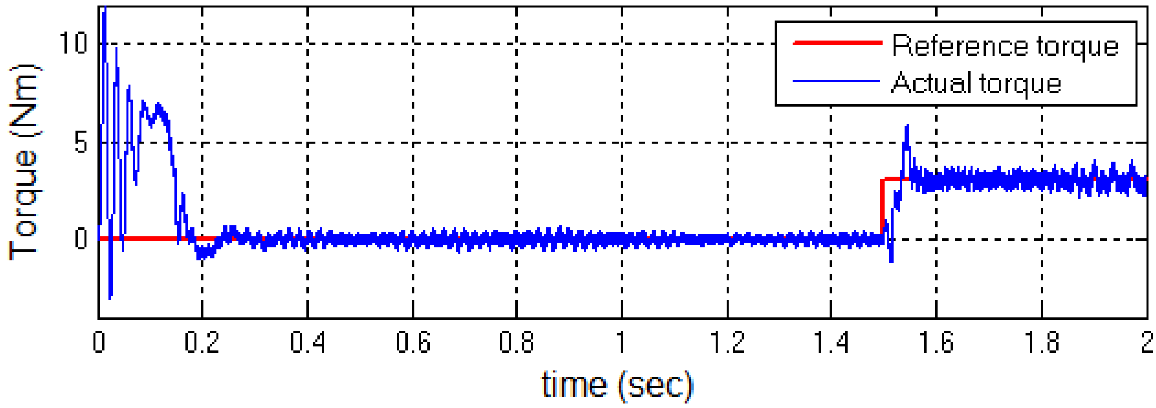

Fig.4.16. Variation of torque for the induction motor.

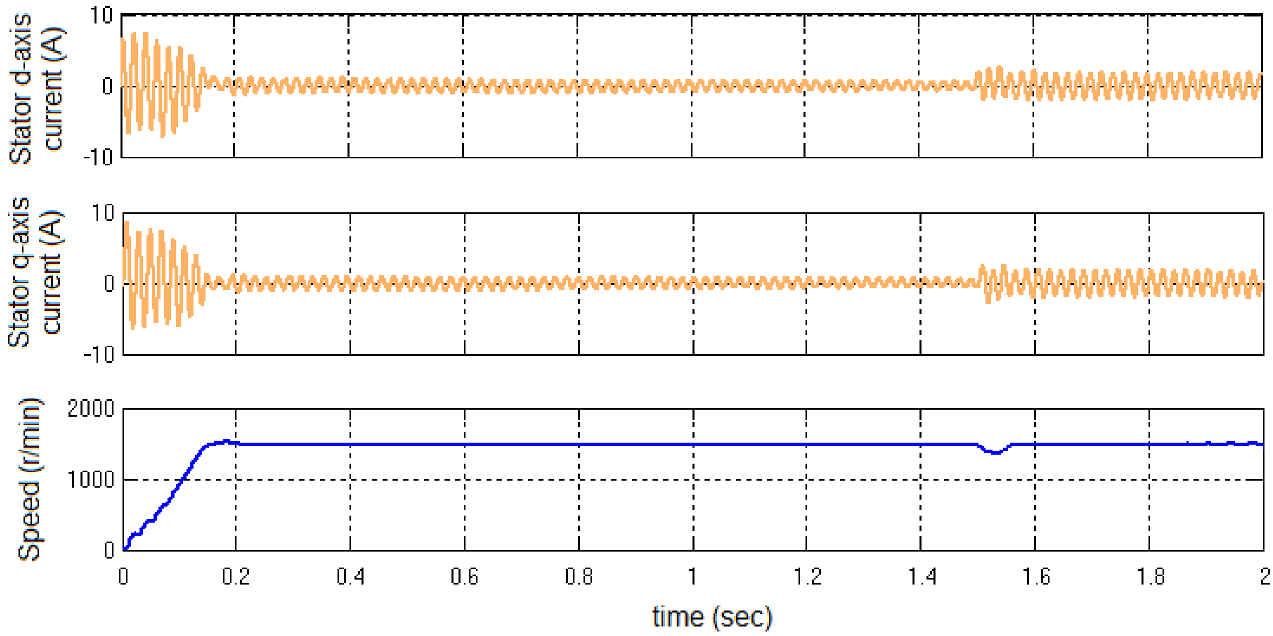

(a)

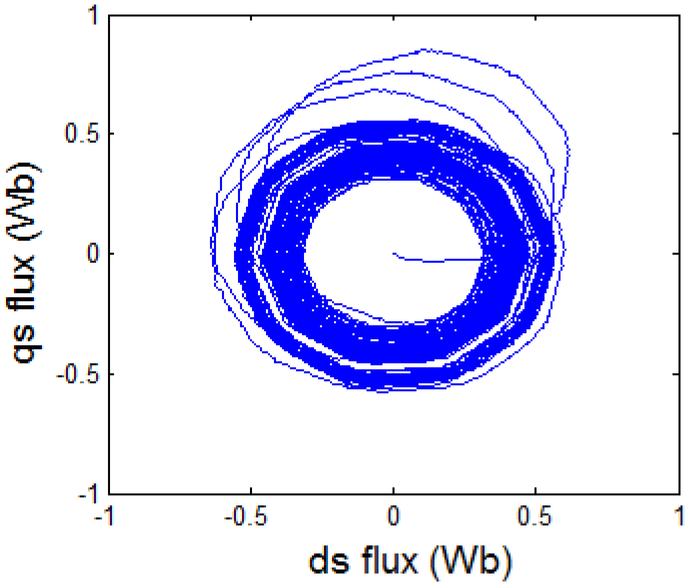

(b)

Fig.4.17. (a) stator currents and the speed with IFOC at varying load and constant speed (b) flux trajectory for the same.

As observed from the simulation results, with higher load, the stator currents are increased and thus the flux is increased as shown by the outer circle of the flux trajectory. At about t = 1.5 sec, the load is increased to 3 Nm and thus the current is increased with an outer circular trajectory as shown in Fig.4.17 (b). Over the whole operating range the machine speed is shown to be at a constant value as set by the external speed reference.

In Fig.4.15 (a) and Fig 4.17(a), while varying the speed reference at constant load torque or vice-versa, here is a sudden dip in speed (or toque) at time t = 2 sec (Fig.4.15 (a)) and t= 1.5sec (Fig.4.17. (a)) because the system is influenced by uncertainties, which usually composed of unpredictable variations in the machine parameters, external load disturbances and modeled and non-linear dynamics.

CHAPTER 5

5. Conclusions and future scope

5.1 Conclusions

In this thesis, IFOC based five-phase induction motor drive is implemented. Initially, the dynamic model (*d*-*q* model) in state space form is developed for transient analysis of induction motor particularly for computer simulation study in *MATLAB/Simulink*. The motor can be modeled in rotating reference frame and stationary frame. The electrical variables in the model are chosen as fluxes, currents, and voltages for simulation modeling. Latter on for speed control, a voltage source inverter (VSI) is used for five-phase supply to induction machine. In a machine drive system, Hysteresis Current Control scheme is done as control of machine current is important because it influences the flux and developed torque directly. High performance drives invariably require current control.

The simulation indicated good performance, good efficiency, less current per phase and smooth torque. The speed and torque ripple are small at steady state. A simple and straightforward approach to the indirect FOC of a five-phase induction machine has been presented. The validity of the scheme was verified by several informative simulation results. The key features of the scheme are the following:

• It is based on a two-axes (*d*-*q*) model of the five-phase machine that can be easily extended to any multiple number of phases as per requirement.

• The *d*-*q* model of the machine and FOC provide the scope for extension of the scheme for operation and control of multiphase induction machines even under fault condition with little modification in the modeling and can calculate torque and speed pulsation during post fault. In general, no separate machine model and control scheme is required for operation under fault condition.

• The stator currents are independently controlled. Thus the problem of unbalance current sharing is eliminated.

Using IFOC methods, faster response of stator fluxes is done. Thus conclude that vector control is rapid and robust compare to scalar control (a sluggish control).

The main disadvantage is complexity and cost of driver circuit is high. Nevertheless it is a high performance control technique.

5.2 Future scope

Multiphase machine systems have attracted much attention in recent past both for power transmission and electric motor drives application. In 21st century, there is a rapid growth of multiphase induction machine and its control strategy. Multiphase machines along with control electronics are design as a system. They are ideally suitable for high power application like marine application, hybrid vehicles, etc. as fault tolerance, high efficiency, low noise are the prime requirement. Variable speed multiphase drive will gain industrial acceptance in future.

For future research using multiphase induction machine drives, the following areas can be explored,

- Rather than vector filed control and direct torque control schemes, one can control the multiphase induction motor drive using sensor-less speed control and fuzzy logic based control using DSP a smooth operation can be performed, etc.
- Operation of the machine under fault condition (more than one phase) can be implementing in future and response of torque and speed can be evaluated.
- Synchronous current controller can be used instead of hysteresis band PWM current control. In hysteresis current control method, its harmonic content is not optimum.

Besides, at higher speeds, the current controller will tend to saturate because of higher back emf. In this condition the fundamental current magnitude and its phase will lose tracking with the command current. Thus vector control will not be valid. All these problems can be solved in a synchronous current controller.

- Application of multi-phase generator in power transmission can be topic of research in future, because supply from grid prone to unbalance and the effect of these unbalanced factors on parameter like efficiency, power factor, stator copper loss can be investigated.
- To provide better control in the presence of such uncertainties (variation of machine parameters, external loads, etc) PI controller can be replaced by other robust control techniques, such as optimal control, Variable structure control, Adaptive, Fuzzy and neural control.

REFERENCES

[1] S.A. Nasar and I. Boldea, The Induction Machine Handbook, CRC Press, London, 2002.

[2] R. Krishnan, “Electric Motor Drives –Modeling, Analysis and Control” PHI Learning Private Limited, New Delhi (2010)

[3] Bimal K. Bose, Modern power electronics and ac drives, Prentice Hall 2002.

[4] G. Kron, “Equivalent Circuits of Electric Machinery,” Wiley (1951).

[5] A.M. Trzynadlowski, The field oriented Principle in Control of Induction motors, Kuluwer Press, 1994.

[6] I. Boldea and S.A. Nasar, Vector Control of AC Drives, CRC Press, London, 1992.

[7] H.A. Toliyat, DSP based Electromechanical Motion Control, CRC Press, 2003.

[8]J. W. Kelly, E. G. Strangas, and J. M. Miller, “Multiphase inverter analysis,” in Proc. IEEE IEMDC, 2001, pp. 147–155.

[9] E. E. Ward and H. Härer, “Preliminary investigation of an inverter-fed 5-phase induction motor,” Proc. Inst. Electr. Eng., vol. 116, no. 6, pp. 980–984, Jun. 1969.

[10] M. A. Abbas, R. Christen, and T. M. Jahns, “Six-phase voltage source inverter driven induction motor,” IEEE Trans. Ind. Appl., vol. IA-20, no. 5, pp. 1251–1259, Sep./Oct. 1984.

[11] K. N. Pavithran, R. Parimelalagan, and M. R. Krishnamurthy, “Studies on inverter-fed five-phase induction motor drive,” IEEE Trans. Power Electron., vol. 3, no. 2, pp. 224–235, Apr. 1988.

[12] E. Andrese and K. Bieniek, “6-phase induction motors for current-source inverter drives,” in Conf. Rec. IEEE IAS Annu. Meeting, Philadelphia, PA, 1981, pp. 607–618.

[13] K. Gopakumar, S. Sathiakumar, S. K. Biswas, and J. Vithayathil, “Modified current source inverter fed induction motor drive with reduced torque pulsations,” Proc. Inst. Electr. Eng., vol. 131, no. 4, pt. B, pp. 159–164, Jul. 1984.

[14] J. Dente and F. Labrique, “Induction motor-current source inverter systems with phase number greater than 3,” in Proc. EPE, Brussels, Belgium, 1985, pp. 3.143–3.147.

[15] T. McCoy and M. Bentamane, “The all electric warship: An overview ofthe U.S. Navy’s integrated power system development programme,” in Proc. Int. Conf. ELECSHIP, Istanbul, Turkey, 1998, pp. 1–4.

[16] M. Benatmane and T. McCoy, “Development of a 19 MW PWM converter for U.S. Navy surface ships,” in Proc. Int. Conf. ELECSHIP, Istanbul, Turkey, 1998, pp. 109–113.

[17] C. Hodge, S. Williamson, and A. C. Smith, “Direct drive marine propulsion motors,” in Proc. Int. Conf. Electrical Machines (ICEM), Bruges, Belgium, 2002, CD-ROM, Paper 807.

[18] S. Smith, “Developments in power electronics, machines and drives,” IEE Power Eng. J., vol. 16, no. 1, pp. 13–17, Feb. 2002.

[19] F. Terrien, S. Siala, and P. Noy, “Multiphase induction motor sensorless control for electric ship propulsion,” in Proc. IEE PEMD Conf., Edinburgh, U.K., 2004, pp. 556–561.

[20] C. L. Ferreira and R. W. G. Bucknall, “Modelling and real-time simulation of an advanced marine full-electrical propulsion system,” in Proc. IEE PEMD Conf., Edinburgh, U.K., 2004, pp. 574–579.

[21] G. K. Singh, “Multi-phase induction machine drive research—A survey,” Electr. Power Syst. Res., vol. 61, no. 2, pp. 139–147, Mar. 2002.

[22] M. Jones and E. Levi, “A literature survey of state-of-the-art in multiphase AC drives,” in Proc. UPEC, Stafford, U.K., 2002, pp. 505–510.

[23] R. Bojoi, F. Farina, F. Profumo, and A. Tenconi, “Dual-three phase induction machine drives control—A survey,” IEEJ Trans. Ind. Appl., vol. 126, no. 4, pp. 420–429, 2006.

[24] E. Levi, R. Bojoi, F. Profumo, H. A. Toliyat, and S. Williamson, “Multiphase induction motor drives—A technology status review,” IET Electr. Power Appl., vol. 1, no. 4, pp. 489–516, Jul. 2007.

[25] E. Levi, “Multi-phase Machines for Variable speed applications” IEEE Trans. Ind. Elect., vol. 55, no. 5, pp. 1893- 1909, May 2008.

[26] L. Zheng, J.E. Fletcher, B.W. Williams and X. He, “Dual-plane vector control of five-phase induction machine for an improved flux pattern”, IEEE Trans. On Ind. Elect., vol. 55, no. 5, pp. 1996-2005, May 2008.

[27] H. Xu, H.A. Toliyat and L.J. Peterson, “Five-phase induction motor with DSP based control system”, IEEE Trans. Power Elect., vol. 17, no. 4, pp. 524-533, Jul. 2002.

[28] G. K. Singh, K. Nam, and S. K. Lim, “A simple indirect field-oriented control scheme for multiphase induction machine,” IEEE Trans. Ind. Electron., vol. 52, no. 4, pp. 1177–1184, Aug. 2005.

[29] G. K. Singh, D. K. P. Singh, K. Nam, and S. K. Lim, “A simple indirect field-oriented control scheme for multiconverter-fed induction motor,” IEEE Trans. Ind. Electron., vol. 52, no. 6, pp. 1653–1659, Dec. 2005.

[30] H. A. Toliyat, T. A. Lipo, and J. C. White, “Analysis of a concentrated winding induction machine for adjustable speed drive applications— Part II: Motor design and performance,” IEEE Trans. Energy Convers., vol. 6, no. 4, pp. 684–692, Dec. 1991.

[31] R. Lyra and T. A. Lipo, “Torque density improvement in a six-phase induction motor with third harmonic current injection,” IEEE Trans. Ind. Appl., vol. 38, no. 5, pp. 1351–1360, Sep./Oct. 2002.

[32] H. Xu, H. A. Toliyat, and L. J. Petersen, “Rotor field oriented control of five-phase induction motor with the combined fundamental and third harmonic currents,” in Proc. IEEE APEC, 2001, vol. 1, pp. 392–398.

[33] H. Xu, H. A. Toliyat, and L. J. Petersen, “Five-phase induction motor drives with DSP-based control system,” IEEE Trans. Power Electron., vol. 17, no. 4, pp. 524–533, Jul. 2002.

[34] H.-M. Ryu, J.-W. Kim, and S.-K. Sui, “Synchronous-frame current control of multiphase synchronous motor under asymmetric fault condition due to open phases,” IEEE Trans. Ind Appl., vol. 42, no. 4, pp. 1062–1070, Jul./Aug. 2006.

[35] L. Parsa and H. A. Toliyat, “Fault-tolerant interior-permanent-magnet machines for hybrid electric vehicle applications,” IEEE Trans. Veh. Technol., vol. 56, no. 4, pp. 1546–1552, Jul. 2007.

[36] N. Bianchi, S. Bolognani, and M. D. Pre, “Strategies for the fault-tolerant current control of a five-phase permanent-magnet motor,” IEEE Trans. Ind. Appl., vol. 43, no. 4, pp. 960–970, Jul./Aug. 2007.

[37] E. Levi, M. Jones, S. N. Vukosavic, and H. A. Toliyat, “A novel concept of a multiphase, multimotor vector controlled drive system supplied from a single voltage source inverter,” IEEE Trans. Power Electron., vol. 19, no. 2, pp. 320–335, Mar. 2004.

[38] K. K. Mohapatra, R. S. Kanchan, M. R. Baiju, P. N. Tekwani, and K. Gopakumar, “Independent field-oriented control of two split-phase induction motors from a single six-phase inverter,” IEEE Trans. Ind. Electron., vol. 52, no. 5, pp. 1372–1382, Oct. 2005.

[39] E. Levi, M. Jones, A. Iqbal, S. N. Vukosavic, and H. A. Toliyat, “Induction machine/syn-rel two-motor five-phase series-connected drive,” IEEE Trans. Energy Convers., vol. 22, no. 2, pp. 281–289, Jun. 2007.

[40] E. Levi, M. Jones, S. N. Vukosavic, A. Iqbal, and H. A. Toliyat, “Modeling, control, and experimental investigation of a five-phase series connected two-motor drive with single inverter supply,” IEEE Trans. Ind. Electron., vol. 54, no. 3, pp. 1504–1516, Jun. 2007.

[41] Z.M.S. El-Barbary, “Fuzzy logic based controller for five-phase induction motor drive system”;Alexandria Engineering Journal (2012) 51, pp. 263–268.

[42] H. A. Toliyat, M. M. Rahinian, Thomas A. Lipo, “dq modeling of Five phase Synchronous Reluctance Machine including Third harmonics of Air-gap MMF”, Research Report, University of Wisconsin-Madison, May 1991.

[43] L. Zheng, J.E. Fletcher, B.W. Williams and X. He, “Dual-plane vector control of five-phase induction machine for an improved flux pattern”, IEEE Trans. On Ind. Elect., vol. 55, no. 5, pp. 1996-2005, May 2008.

[44] G.K. Singh, M. Bhattacharyya, V. Pant “, Improved reliability and high power rating in ac drives by means of phase redundancy—some analytical and experimental results, Journal of Institution of Engineers (India) 82 (2001), pp. 7–14.

[45] V. Pant, G.K. Singh, S.N. Singh, “ Modeling of a multiphase induction machine under fault condition, in: Proceedings IEEE The Third International Conference on Power Electronics and Drive Systems, PEDS’99, Hong Kong, July 26– 29, 1999, Vol. 1, pp. 92–97.

[46] G.K. Singh, V. Pant, “Analysis of multiphase induction machine under fault condition in a phase-redundant ac drive system”, Int. J. Electric Machines Power Syst. 28 (6) (2000), pp. 577–590.

[47] MATLAB/Simulink Toolbox User’s Guide, The Math works Inc., Natick, MA, USA, May 1998.